

Identification of Paired-related Homeobox Protein 1 as a key mesenchymal transcription factor in Idiopathic Pulmonary Fibrosis

E. Marchal-Duval^{1,*}, M. Homps-Legrand^{1,*}, A. Froidure^{1,2}, M. Jaillet¹, M. Ghanem³, L. Deneuille^{1,3}, A. Justet^{1,3}, A. Maurac¹, A. Vadel¹, E. Fortas¹, A. Cazes^{1,4}, A. Joannes^{1,5}, L. Giersch¹, H. Mal⁶, P. Mordant^{1,7}, C.M. Mounier^{8,9}, K. Schirduan¹⁰, M. Korfei¹¹, A. Gunther¹¹, B. Mari⁸, F. Jaschinski¹⁰, B. Crestani^{1,3}, A.A. Mailleux^{1,\$}

¹ Institut National de la Santé et de la Recherche Médicale, UMR1152, Labex Inflammex, DHU FIRE, Université de Paris, Faculté de médecine Xavier Bichat, 75018 Paris, France;

² Institut de Recherche Expérimentale et Clinique, Pôle de Pneumologie, Université catholique de Louvain, Belgium Service de pneumologie, Cliniques Universitaires Saint-Luc, Brussels, Belgium;

³ Assistance Publique des Hôpitaux de Paris, Hôpital Bichat, Service de Pneumologie A, DHU FIRE, Paris, France ;

⁴ Assistance Publique des Hôpitaux de Paris, Hôpital Bichat, Département d'Anatomopathologie, DHU FIRE, Paris, France ;

⁵ Univ Rennes, Inserm, EHESP, Irset (Institut de recherche en santé, environnement et travail) - UMR_S 1085, F-35000 Rennes, France

⁶ Assistance Publique des Hôpitaux de Paris, Hôpital Bichat, Service de Pneumologie et Transplantation, DHU FIRE, Paris, France ;

⁷ Assistance Publique des Hôpitaux de Paris, Hôpital Bichat, Service de Chirurgie Thoracique et Vasculaire, DHU FIRE, Paris, France ;

⁸ Université Côte d'Azur, CNRS, IPMC, FHU-OncoAge, Valbonne, France

⁹ CYU Université, ERRMECe(EA1391), NEUVILLE SUR OISE, France

¹⁰ Secarna Pharmaceuticals GmbH & Co. KG – Planegg/Martinsried (Germany)

¹¹ Department of Internal Medicine II, University of Giessen-Marburg Lung Center, Justus-Liebig University Giessen, Giessen, Germany.

* Both authors equally contributed to this manuscript.

\$ corresponding author: Dr. Arnaud Mailleux, INSERM, U1152, 16 rue Henri Huchard 75018, Paris, France. E-mail: arnaud.mailleux@inserm.fr; Phone: (33)157277584; Fax: (33)157277551

“The authors have declared that no conflict of interest exists.”

Brief Summary

Inhibition of a single fibroblast-associated transcription factor, namely paired-related homeobox protein 1, is sufficient to dampen lung fibrogenesis.

Keywords: lung fibrosis, IPF, transcription factor, mesenchyme, fibroblast, bleomycin.

ABSTRACT:

Matrix remodeling is a salient feature of idiopathic pulmonary fibrosis (IPF). Targeting cells driving matrix production and remodeling could be a promising avenue for IPF treatment. Analysis of public transcriptomic database identified paired-related homeobox protein-1 (PRRX1) as an upregulated mesenchymal transcription factor (TF) in IPF. We confirmed that *PRRX1* isoforms were upregulated in IPF lung tissue and strongly expressed by lung fibroblasts.

In vitro, *PRRX1* expression was up-regulated by cues associated with proliferative and anti-fibrotic properties in lung fibroblasts, while IPF fibroblast-derived matrix increased *PRRX1* TFs expression in a PDGFR dependent manner in control ones. Meanwhile, signals promoting myofibroblastic differentiation decreased *PRRX1* TF.

We demonstrated that *PRRX1* inhibition decreased fibroblast proliferation by downregulating the expression of S phase cyclins. *PRRX1* inhibition also impacted TGF- β driven myofibroblastic differentiation by inhibiting SMAD2/3 phosphorylation through phosphatase PPM1A upregulation and TGFR2 downregulation, leading to a TGF- β response global decrease.

Finally, targeted inhibition of *Prrx1* TFs attenuated fibrotic remodeling both in vivo with intra-tracheal antisense oligonucleotides in the bleomycin mice model of lung fibrosis and ex vivo using mouse and Human precision-cut lung slices stimulated with fibrosis cytokine cocktail.

Altogether, our results identified *PRRX1* as a mesenchymal transcription factor driving myofibroblastic phenotype and lung fibrogenesis.

INTRODUCTION:

Chronic remodeling is a key feature of many Human diseases associated with aging. In particular, chronic respiratory diseases, including lung fibrosis, are a major and increasing burden in terms of morbidity and mortality¹. For instance, idiopathic pulmonary fibrosis (IPF) is the most common form of pulmonary fibrosis. IPF is defined as a specific form of chronic, progressive fibrosing interstitial pneumonia of unknown cause. IPF patients have an overall median survival of 3 to 5 years¹.

According to the current paradigm, IPF results from progressive alterations of alveolar epithelial cells leading to the recruitment of mesenchymal cells to the alveolar regions of the lung with secondary deposition of extracellular matrix, and destruction of the normal lung structure and physiology. IPF develops in a susceptible individual and is promoted by interaction with environmental agents such as inhaled particles, tobacco smoke, inhaled pollutants, viral and bacterial agents. Aging is probably both a susceptibility marker and a major driver of the disease, through mechanisms that are not yet fully elucidated. Two drugs (Pirfenidone and Nintedanib) appear to slow disease progression and may improve long term survival¹.

Among the multifaceted tissue cellular “ecosystem”, cells of mesenchymal origin are the main cellular components responsible for tissue remodeling during normal and pathological lung tissue repair^{1,2}. On one hand, the interactions between the mesenchymal cells and the epithelial compartment are disturbed as a consequence of the aberrant reactivation of developmental pathways in IPF^{2,3}. On the other hand, a growing body of evidence has also demonstrated that there are intrinsic phenotypic and behavioral differences between mesenchymal lung cells derived from healthy donor and patients with IPF^{1,2}. In any given cell, a set of transcription factors is expressed and works in concert to govern cellular homeostasis and function. Dysregulation of transcriptional networks may therefore account to those aberrant phenotypic changes observed in IPF fibroblasts.

Using an *in silico* approach, we screened publicly available transcript microarray databases for expression of mesenchyme-associated transcription factors in control and IPF lung samples. We identified the “Paired Related Homeobox Protein-1” (*PRRX1*) gene as a potential candidate for transcriptional regulation differently modulated in IPF compared to control lungs. The *PRRX1* mRNA generates by alternative splicing two proteins, PRRX1a (216 aa) and PRRX1b (245 aa) that differ at their C-terminal parts. Functional *in vitro* studies suggested that PRRX1a promoted transcriptional activation whereas PRRX1b may act rather as a transcriptional repressor⁴.

Prrx1 is implicated in the regulation of mesenchymal cell fate during embryonic development. PRRX1 is essential for fetal development as *Prrx1*^{-/-} mice present severe malformation of craniofacial, limb, and vertebral skeletal structures⁵. *Prrx1*^{-/-} mice also display

hypoplastic lungs with severe vascularization defects and die soon after birth ⁶. PRRX1 function is not restricted to embryogenesis. It has been also shown that PRRX1 was a stemness regulator ⁷, involved in adipocyte differentiation ⁸, epithelial tumor metastasis and pancreatic regeneration ^{9–11} as well as liver fibrosis ¹². Other studies indicate that PRRX1 transcription factors are at the center of the network coordinating dermal fibroblast differentiation ¹³. A *Prrx1* positive fibroblast subpopulation was recently characterized as pro-fibrotic in the mouse ventral dermis ^{14,15}. Interestingly, *Prrx1* mRNA expression was also associated with a sub-population of matrix fibroblast in the bleomycin experimental mouse model of lung fibrosis using single-cell RNA sequencing ¹⁶. PRRX1 expression was also recently reported in the fibroblast foci in IPF lung ¹⁷.

However, whether and how PRRX1 plays a role in lung fibrogenesis still remains elusive. Given its central position in fibroblast transcriptional network, it could constitute a promising target for future treatments. We hypothesized that PRRX1 transcription factors are important drivers of the aberrant phenotype of fibroblasts in IPF, promoting the development/progression of fibrosis.

In this study, we first depicted in detail the expression pattern and levels of PRRX1 TF isoforms in whole lung samples and primary lung cell types obtained from control subjects and from patients with IPF; secondly we deciphered the regulation of PRRX1 expression levels by soluble mediators and extracellular microenvironment; finally, we evaluated the phenotypic consequences of the inhibition of PRRX1 TFs in control and IPF primary lung fibroblasts as well as the anti-fibrotic potential of PRRX1 TFs inhibition in an experimental mouse model of lung fibrosis and ex vivo using Human and mouse precision-cut lung slices (PCLS).

RESULTS:

Identification of *PRRX1* isoforms as mesenchymal transcription factors associated with IPF.

Since mesenchymal cells are thought to be one of the major effector cells during fibrosis^{1,2}, we sought to identify mesenchymal transcription factors associated with IPF in patients. We screened three curated publicly available transcript microarray databases from NCBI GEO (GDS1252, GDS4279, GDS3951) for transcription factor expression in IPF and control whole lung samples. Among the 210 common genes upregulated at the mRNA level in all three IPF lung datasets compared to their respective control ones (Figure 1A and supplemental Table S1), 12 genes were annotated as transcription factors (Figure 1A) after gene ontology analysis. One of these transcription factors, *PRRX1* appeared as an appealing candidate since this gene was previously associated with mesenchymal cell fate during embryogenesis⁵ and is required for proper lung development⁶. In addition, *PRRX1* mRNA was upregulated in a fourth transcriptome dataset comparing “rapid” and “slow” progressor subgroups of IPF patients¹⁸. None of those transcriptome datasets discriminated *PRRX1* isoforms, namely *PRRX1a* and *PRRX1b*.

First, we confirmed that both *PRRX1* isoforms were upregulated in Human IPF lungs at the mRNA and protein levels (Figure 1B-C). Immunoblot revealed that *PRRX1a* protein (210 aa) was the main *PRRX1* isoform expressed in control and IPF lungs. We also investigated *PRRX1* expression pattern by immunohistochemistry in control and IPF Human lung tissue sections (the antibody recognized both *PRRX1* isoforms, see figure 1D). Additional lineage markers were also investigated such as Vimentin (mesenchyme marker), ACTA2 (myofibroblast / smooth muscle marker) and CD45 (hematopoietic lineage) as shown in supplemental Figure S1. *PRRX1* positive cells were not detected in the distal alveolar space and in the bronchiolar epithelium of control lung (Figure 1D). Nevertheless, *PRRX1* nuclear staining was observed in mesenchymal cells (Vimentin positive but ACTA2 and CD45 negative cells) within peri-vascular and peri-bronchiolar spaces (Figure 1D and supplemental Figure S1). In IPF patients, nuclear *PRRX1* positive cells were mainly detected in the fibroblast foci (Figure 1D), which are the active sites of fibrogenesis^{1,2}. Those *PRRX1* positive cells were all Vimentin positive and CD45 negative but only some were expressing ACTA2 (supplemental Figure S1).

Interestingly, fully differentiated mesenchymal cells such as bronchiolar smooth muscle cells were *PRRX1* negative in control and IPF lung paraffin sections (Figure 1D). The remodeled distal epithelium was also *PRRX1* negative in IPF lung samples (Figure 1D), while scattered *PRRX1* positive cells were detected in the underneath stroma.

To confirm the identity of *PRRX1* expressing cells in the lung as fibroblasts, we took advantage of recently published single-cell transcriptomic analysis performed using lung samples^{19,20}.

PRRX1 mRNA expression was restricted to the fibroblast / mesenchymal cell lineages in either lung transplant donors or recipients with pulmonary fibrosis (Figure 2A and supplemental Figure S2).

In vitro, both isoforms, *PRRX1a* and *PRRX1b* mRNA were also found to be strongly expressed by primary lung fibroblasts compared to primary alveolar epithelial type 2 cells (AECII) and alveolar macrophages (Figure 2B) by quantitative PCR (qPCR). In addition, *PRRX1a* and *-1b* mRNA levels were increased in IPF primary lung fibroblasts compared to control ones (Figure 2C). However, the upregulation of *PRRX1* in IPF primary fibroblasts was not confirmed at the protein levels as assayed by western blot (Figure 2D). Finally, *PRRX1* was also detected at the protein level in the nuclei of both control and IPF fibroblasts cultured *in vitro* by immunofluorescence (Figure 2E).

***PRRX1* isoforms expression in primary lung fibroblasts is tightly regulated by growth factors and extracellular matrix *in vitro*.**

To better understand the regulation of *PRRX1* isoforms in lung fibroblasts, we first assayed the effects of known pro- and anti-fibrotic factors on the expression of both *PRRX1* isoforms in control and IPF primary lung fibroblasts. Interestingly, “Transforming growth factor beta 1” (TGF- β 1, 1ng/ml) treatment which triggers myofibroblastic differentiation² was associated with a decrease in the expression level of both *PRRX1* isoforms at the mRNA level (Figure 3A). This effect was confirmed at the protein level by western blot respectively in 8 out of 10 control fibroblasts and 8 out of 11 IPF fibroblasts assayed as well as by immunofluorescence (supplemental Figure S3). Conversely, prostaglandin E₂ (PGE₂, 100nM) treatment which decreases myofibroblastic differentiation² was associated with an increase of *PRRX1* isoforms mRNA and protein in both control and IPF fibroblasts (Figure 3A and supplemental Figure S3). We also assayed the effects of “Fibroblast growth Factor 2” (FGF2, 20ng/ml), which promotes fibroblast proliferation and survival². FGF2 treatment increased the expression of both *PRRX1* isoforms in both control and IPF fibroblasts at the mRNA and protein levels (Figure 3A and supplemental Figure S3). In the meantime, stimulation of both control and IPF primary lung fibroblasts with “Platelet derived growth factors” such as PDGF-AA or PDGF-BB (10ng/ml) did not significantly change *PRRX1* isoforms mRNA in those cells (supplemental Figure S4). PDGF-A selectively binds to the PDGFR α receptor, while PDGF-B chain isoforms can bind to either PDGFR α or PDGFR β receptors²¹

Concomitantly with an aberrant growth factors/chemokine secretory profile, lung fibrosis is also characterized by local matrix stiffening, which plays a key role in IPF physiopathology²². Control and IPF primary lung fibroblasts were cultured on fibronectin-coated glass (elastic/Young’s modulo in the GPa range) or hydrogel substrates of discrete stiffness, spanning the range of normal (1.5kPa) and fibrotic (28kPa) lung tissue²². The

expression levels of both *PRRX1* TFs isoforms mRNA were increased on soft/normal 1.5kPa stiffness substrate (Figure 3B) compared to stiff substrates (Glass and 28kPa culture conditions). Previous studies²³ showed that increasing matrix stiffness strongly suppresses fibroblast expression of *PTGS2*, a key enzyme in PGE₂ synthesis. First, we confirmed that soft (1.5kPa) substrate culture condition did increase *PTGS2* mRNA level compared to stiff/glass control condition in both control and IPF fibroblasts (supplemental Figure S4). Treatment with NS398 (10µg/ml), a specific *PTGS2* inhibitor abrogated the *PRRX1* TFs increase on soft substrate (Figure 3C). On the other hand, Rho kinase activity is known to increase with matrix stiffness²⁴, contributing to myofibroblastic differentiation. Conversely, Fasudil (35µM), an inhibitor of ROCK1 and ROCK2, is known to counteract myofibroblastic differentiation on stiff substrate²⁴. We found that inhibition of mechanosensitive signalling with Fasudil treatment induced *PRRX1* TFs mRNA expression in both control and IPF fibroblasts grown on glass/stiff substrate (Figure 3C).

We also investigated the effect of tridimensional (3D) microenvironments on *PRRX1* TFs expression levels in lung fibroblasts using natural, cell-derived 3D extracellular matrices (ECM). We used control and IPF fibroblasts in high-density culture to generate thick matrices that were extracted with detergent at alkaline pH to remove cellular contents (Figure 3D). This treatment leaves behind a 3D ECM that is intact and cell-free²⁵. Our results showed that *PRRX1a* and *-1b* TF mRNA expression levels in control fibroblasts are only upregulated on IPF fibroblast derived 3D ECM compared to plastic culture (Figure 3E). Meanwhile, *PRRX1a* and *-1b* mRNA expression levels were stable in IPF fibroblasts seeded either on control or IPF fibroblast derived 3D ECM compared to plastic culture (Figure 3E).

To better understand the cellular processes and signalling pathways involved, control fibroblasts seeded on IPF fibroblast-derived matrix were treated with two tyrosine kinase protein inhibitors, namely Imatinib (10µg/ml) and Nintedanib (10nM). Those tyrosine kinase inhibitors have anti-fibrotic properties on lung fibroblasts²⁶ and Nintedanib is one of the two drugs currently approved for IPF treatment¹. Both inhibitors reverted the effect of IPF fibroblast-derived matrix upon *PRRX1a* and *PRRX1b* mRNA levels (Figure 3E). Interestingly, amongst their multiple targets^{1,2}, Imatinib and Nintedanib are known to both inhibit PDGFR. The treatment of control lung fibroblasts seeded on IPF fibroblast-derived matrix with the small inhibitory molecule PDGFR V at the nanomolar range (10nM) did confirm the PDGFR-dependency of this effect (Figure 3E). Similarly to plastic culture condition, treatment with recombinant PDGF-AA or PDGF-BB (10ng/ml) of control fibroblasts seeded on control fibroblast derived 3D ECM did not recapitulate the effect of IPF lung fibroblast derived 3D ECM since *PRRX1a* or *-1b* mRNA expression levels were not upregulated compared to plastic condition (Supplemental Figure S4). To investigate a potential PDGF autocrine feedback loop, *PDGFA* and *PDGFB* mRNA levels were also assayed in control lung fibroblasts seeded on IPF

lung fibroblast derived 3D ECM compared to control fibroblast derived 3D ECM and plastic conditions (Supplemental Figure S4). There was neither upregulation nor differential regulation of *PDGFA* or *PDGFB* mRNA levels in control lung fibroblasts cultured on control or IPF fibroblast derived 3D ECM compared to plastic basal condition (Supplemental Figure S4). Similar results were obtained regarding *PDGFC* and *PDGFD* mRNA expression levels (data not shown). Altogether, these results suggested a ligand-independent activation of PDGFR may be involved in the effect of IPF fibroblast 3D ECM on *PRRX1a* and *-1b* mRNA levels in control fibroblasts.

In conclusion, *PRRX1* expression was up-regulated by cues associated with proliferative and anti-fibrotic properties in lung fibroblasts (FGF2, PGE2 and soft culture substrate), while IPF fibroblast-derived matrix also increased *PRRX1* TFs expression only in control fibroblasts in a PDGFR dependent manner. Meanwhile, signals promoting myofibroblastic differentiation, decreased *PRRX1* TF expression levels (TGF- β 1 and stiff culture substrate).

PRRX1 TF isoforms promote fibroblast proliferation.

Since *PRRX1* expression is strongly associated with fibroblasts in IPF, we next investigated whether *PRRX1* TFs may drive the phenotype of primary lung fibroblasts. The involvement of *PRRX1* was studied in vitro by using siRNA targeting both *PRRX1a* and *PRRX1b* isoforms (loss of function).

First, we investigated the effects of *PRRX1* TFs knock down using two different siRNA sequences (see Figure 4A-B showing high knock down efficiency at both mRNA and protein levels compared to control siRNA at 72h). Knockdown of *PRRX1* TFs significantly decreased primary lung fibroblast proliferation in complete growth medium after 72h (Figure 4C) as compared to the control siRNA. Cell cycle analysis by FACS (measurement of DNA content with PI) revealed a significant decrease in S phase concomitantly with an increase in G1 phase, suggestive of a G1/S arrest in control and IPF lung fibroblasts treated with *PRRX1* siRNA (Figure 4D and supplemental Figure S5). This potential G1/S arrest was also associated with a strong decrease in *CCNA2* and *CCNE2* mRNA expression after 72 hours (Figure 4E). These two cyclins play a key role in the replicative S phase during the cell cycle²⁷. To further characterize the impact of *PRRX1* TF inhibition on cell cycle progression, we performed a FACS analysis of KI67 expression in primary control and IPF lung fibroblasts transfected with *PRRX1* siRNA sequences for 72h compared to control siRNA. KI67 protein is usually present during all active phases of the cell cycle, but is absent from resting cells in G0²⁸. *PRRX1* inhibition strongly decreased the number of KI67 (*MKI67*; official name) positive cells in control and IPF lung fibroblasts (Figure 4F and supplemental Figure S5). Of note, *MKI67* expression

was also decreased at the mRNA level in control and IPF lung fibroblasts treated with *PRRX1* siRNA (supplemental Figure S5). Next, we used a chromatin immunoprecipitation approach (ChIP) to assay a possible direct regulatory effect of *PRRX1* upon *CCNA2*, *CCNE2* and *MKI67* gene loci in primary normal Human lung fibroblasts (NHLF). We observed an enrichment of *PRRX1* binding at the vicinity of *PRRX1* response element (*PRE*) identified in the *CCNA2*, *CCNE2* and *MKI67* promoter regions. Meanwhile, no *PRRX1* binding was detected at the *GAPDH* transcription starting site (TSS); devoid of *PRE* (Figure 4G).

We also assayed the effect of *PRRX1* knock down on the mRNA expression of *CDKN2A* (p16), *CDKN1A* (p21) and *TP53*, major negative regulators of cell cycle also associated with cellular senescence²⁷. The expression of all three cell cycle inhibitors was increased only at the mRNA level in both control and IPF lung fibroblasts treated with *PRRX1* siRNA compared to control siRNA as assayed by qPCR and western blot (see supplemental Figure S5 and data not shown). This cell cycle arrest in control and IPF lung fibroblasts treated with *PRRX1* siRNA was not associated with an increase in β -Galactosidase activity, a senescence marker, compared to cells transfected with control siRNA (data not shown).

In conclusion, our results showed that *PRRX1* controlled fibroblast proliferation in vitro.

***PRRX1* TFs are required for the induction of alpha smooth muscle actin during TGF- β 1-driven myofibroblastic differentiation.**

We also investigated the effects of *PRRX1* TFs partial loss of function on myofibroblastic differentiation in primary control and IPF lung fibroblasts. In an appropriate microenvironment, fibroblasts can differentiate by acquiring contractile properties (such as expression of alpha smooth muscle actin (*ACTA2*); gamma smooth muscle actin (*ACTG2*) and Transgelin (*TAGLN / SM22*)) and becoming active producers of extracellular matrix (ECM) proteins (such as Collagen 1, *COL1*; Fibronectin, *FN1*; Tenascin C, *TNC* and Elastin, *ELN*). Aberrant activation of fibroblasts into myofibroblasts is thought to be a major driver of lung fibrogenesis^{1,2}.

First, we evaluated the effects of *PRRX1* modulation on the expression of myofibroblast markers such as *ACTA2*, *COL1* and *FN1* at basal condition. *PRRX1* TF loss of functions robustly did not modify the basal expression of these markers at the mRNA and proteins levels after 48h of treatment as assayed respectively by qPCR and western blot (supplemental Figure S6). *PRRX1* has been implicated in a positive feed-back loop in which *TWIST1* directly increased *PRRX1* which subsequently induced Tenascin-C that itself stimulated *TWIST1* activity in Cancer associated fibroblast (CAF), dermal and fetal Human lung fibroblast lines¹⁷. However, we observed that *PRRX1* inhibition with siRNA failed to modulate *TNC* and *TWIST1* mRNA levels in adult primary control and IPF lung fibroblasts (supplemental Figure S6).

Next, we determined whether *PRRX1* TFs may regulate myofibroblastic differentiation

upon TGF- β 1 stimulation. Control and IPF primary lung fibroblasts were first treated with *PRRX1* siRNA for 48h and then stimulated with 1ng/ml of TGF- β 1 for 48h. The inhibition of *PRRX1* TFs impacted the upregulation of contractile-associated actin isoforms at the mRNA levels such as *ACTA2* (α -SMA) and *ACTG2* (γ -SMA) in response to TGF- β 1 stimulation (Figure 5A and supplemental Figure S7). The expression of the actin binding protein *TAGLN* (*SM22*) was not perturbed (supplemental Figure S7). The effect of *PRRX1* inhibition upon *ACTA2* upregulation was confirmed at the protein level in both control and IPF fibroblasts (Figure 5B). We also investigated a possible interaction of *PRRX1* TFs with *ACTA2* gene promoter regions by ChIP in primary NHLF. An enrichment in *PRRX1* TF binding was observed in *ACTA2* loci at the level of a previously reported SRF response element²⁹ and at the level of a more upstream *PRRX* response element (supplemental Figure S7).

With respect to ECM synthesis, *PRRX1* knock down did not change *FN1* or *A1COL1* upregulation after TGF- β 1 stimulation, both at mRNA and protein levels (supplemental Figure S7). Nevertheless, other ECM proteins associated with IPF were modulated after *PRRX1* down regulation in presence of TGF- β 1. For instance, the expression of *TNC* mRNA was increased in *PRRX1* siRNA treated control and IPF lung fibroblasts compared to control siRNA treated one in presence of TGF- β 1 (supplemental Figure S7). Meanwhile, the expression of *ELN* mRNA was significantly downregulated only in IPF lung fibroblasts (supplemental Figure S7) after TGF- β 1 stimulation.

***PRRX1* TFs modulate SMAD2 and SMAD3 phosphorylation in response to TGF- β 1 by regulating the expression of TGF β Receptor 2 (TGFBR2) and the serine/ threonine phosphatase PPM1A.**

To decipher the mechanism underlying the effects of *PRRX1* downregulation during TGF- β 1 induced myofibroblastic differentiation, we assayed SMAD2 and SMAD3 phosphorylation in control and IPF fibroblasts treated with *PRRX1* siRNA in presence of TGF- β 1 (30min stimulation) compared to cells transfected with control siRNA in presence or absence of TGF- β 1 (Figure 5C). Phosphorylation levels of SMAD2 and SMAD3 were used as activation markers of the canonical TGF- β receptor-mediated signalling pathway. As expected, TGF- β 1 stimulation of control and IPF fibroblasts treated with control siRNA induced a strong phosphorylation of both SMAD2 and SMAD3 compared to unstimulated transfected cells (Figure 5C). In contrast, SMAD2 and SMAD3 phosphorylation levels were strongly inhibited in both control and IPF fibroblasts treated with *PRRX1* siRNA and stimulated with TGF- β 1 for 30 minutes (Figure 5C). On the other hand, the activation of non-canonical/SMAD independent TGF- β receptor-mediated signalling pathway such as AKT and JNK was not impacted by *PRRX1* knock down in both control and IPF fibroblast treated with TGF- β 1 for 30 minutes (data not shown).

First, we investigated the potential effect of *PRRX1* siRNA on the expression of TGF- β 1 receptors. Unlike *TGFBR1* (data not shown), *TGFBR2* expression was downregulated at mRNA and protein levels in both control and IPF fibroblasts treated with *PRRX1* siRNA for 48h compared to control siRNA (Figure 5D and supplemental Figure S7). A ChIP assay was undertaken to investigate a possible interaction of *PRRX1* TFs with *TGFBR2* gene promoter regions. However, no enrichment in *PRRX1* TF binding was detected in *TGFBR2* promoter regions by ChIP in primary NHLF (data not shown).

Among the plethora of phosphatases known to regulate SMAD2 and SMAD3 phosphorylation downstream of TGF- β receptor activation³⁰, we observed that *PRRX1* siRNA-mediated inhibition was associated with an increase of PPM1A, a phosphatase member of the PP2C protein family, at both mRNA and protein levels compared to control and IPF treated with control siRNA for 48h (Figure 5E and supplemental Figure S7). Interestingly, the siRNA-mediated inhibition of *PPM1A* in control and IPF fibroblast treated with *PRRX1* siRNA partially rescued SMAD3 phosphorylation levels after TGF- β 1 stimulation compared to TGF- β 1 stimulated cells transfected only with *PRRX1* siRNA (Figure 5E and supplemental Figure S8). Next, a ChIP assay in primary NHLF was performed to investigate a possible interaction of *PRRX1* TFs with *PPM1A* gene *loci*. Indeed, an enrichment in *PRRX1* TF binding was detected in *PPM1A* promoter regions (supplemental Figure S8).

To better appreciate the *PRRX1* siRNA effects upon TGF- β 1 pathway, whole transcriptome profiling was then performed on NHLF treated with *PRRX1* or control siRNAs in presence or absence of TGF- β 1. In agreement with our data, *PRRX1* knockdown significantly affected *TGFBR2* expression (Figure 5F and supplemental Figure S9). Of note, Ingenuity Pathway Analysis indicated that the most significantly modulated pathway by *PRRX1* inhibition was the TGF- β 1 pathway, which was significantly inhibited in TGF- β -stimulated NHLF treated with *PRRX1* siRNA for 48h compared to control siRNA (Figure 5F, supplemental Figure S9 and supplemental Table S2).

Altogether, our results suggested that *PRRX1* TFs are required to achieve proper myofibroblastic differentiation upon TGF- β 1 stimulation. The effect is at least partially mediated through downregulation of the TGF- β receptor 2 and upregulation of the PPM1A phosphatase. In addition, *PRRX1* knock down led to a global decrease of TGF- β response, as measured at a global scale by whole transcriptome profiling.

PRRX1 TFs expression levels are upregulated in the bleomycin-induced model of lung fibrosis.

In the light of our *in vitro* results regarding *PRRX1* function in Human lung fibroblasts, we investigated whether alteration in *PRRX1* expression may also contribute to fibrogenesis in the bleomycin-induced model of lung fibrosis (single intratracheal instillation³¹). In this

model, the expression levels of both *Prrx1* isoforms mRNA were mainly increased during the fibrotic phase from day 7 compared to the control PBS treated animals (Figure 6A). The upregulation of PRRX1 expression level was confirmed at the protein level only at day 14 during fibrosis phase peak (Figure 6B).

Similarly to control Human lungs, PRRX1 positive cells were detected only within the peri-vascular and peri-bronchiolar spaces in PBS control mice, while the distal alveolar space and the bronchiolar epithelium were devoid of PRRX1 staining as assayed by immunohistochemistry. Meanwhile, PRRX1 positive cells were detected in the remodeled fibrotic area of bleomycin treated animals at day 14 (Figure 6C). In summary, our results indicated that PRRX1 TFs upregulation was associated with fibrosis development in the bleomycin-induced model of lung fibrosis.

In vivo inhibition of PRRX1 dampens lung fibrosis.

Since *Prrx1* loss of function is associated with perinatal lethality in *Prrx1*^{-/-} pups^{5,6,32}, we sought first to evaluate *Prrx1* function during lung fibrosis using *Prrx1*^{+/-} heterozygous mice. Unfortunately, loss of one *Prrx1* allele was not associated with any haploinsufficiency (supplemental Figure S10) and those *Prrx1*^{+/-} heterozygous mice were not protected from lung fibrosis at day 14 after intratracheal instillation of bleomycin (supplemental Figure S10).

In order to evaluate the involvement of PRRX1 TFs in pulmonary fibrosis in vivo, we then chose to treat wild type mice with a third generation antisense LNA-modified oligonucleotide (ASO) targeting both *Prrx1* isoforms (endotracheal route) in the bleomycin-induced model of lung fibrosis from day 7 to day 13 (during the fibrotic phase). As compared to control ASO, *Prrx1* ASO strongly reduced the expression of both *Prrx1* isoforms at the mRNA and protein levels (Figure 7A, B) and reduced the extent of lung lesions on day 14 (Figure 7C). Lung collagen content was decreased as assessed with picrosirius staining, immunohistochemistry and hydroxyproline assay (Figure 7D-F). A similar decrease in ACTA2 staining was observed in *Prrx1* ASO treated animals at day 14 by immunohistochemistry (Figure 7E). In addition, *Prrx1* ASO decreased *Col1a1*, *and *Acta2* mRNA content (Figure 8A) in PRRX1 ASO treated bleomycin mice compared to control ASO treated ones. Finally, the expression levels of COL1, FN1 and ACTA2 were also decreased at the protein level as assayed by Western Blot (Figure 8B-C). The dampened fibrosis development observed in PRRX1 ASO treated bleomycin mice was also associated with a decrease in fibrosis markers such as *Tgfb1* and *Ctgf* as well as inflammatory markers as *Tnf* and *Serp1-1* at the mRNA level (supplemental Figure S11). Furthermore, *Prrx1* was recently identified as the master transcription factor in the *Col14a1* subtype mesenchymal cell during fibrogenesis in this experimental model¹⁶. Interestingly, the expression of *Col14a1* mRNA was also strongly decreased in the *Prrx1* ASO treated animals compared to control ASO at day 14 as assayed*

by qPCR (supplemental Figure S11). With respect to another fibrosis-associated key ECM protein, *Tnc* mRNA level was also decreased in the *Prrx1* ASO treated bleomycin group (supplemental Figure S11).

The expression levels of the proliferation marker *Mki67* was decreased at the mRNA levels in the *Prrx1* ASO treated animals compared to control ASO at day 14 as assayed by qPCR (Figure 8D). A decrease in KI67 positive cells was also observed by immunohistochemistry in the *Prrx1* ASO treated animal lungs after bleomycin challenge compared to control ASO ones at day 14 (Figure 8D).

PRRX1 inhibition attenuates lung fibrosis in mouse and Human precision-cut lung slices (PCLS) treated with a cocktail of fibrosis-associated cytokines and in IPF PCLS.

To confirm the effect of the *Prrx1* ASO in a second model of lung fibrosis, we took advantage of a well-established ex vivo model of lung fibrosis using precision-cut lung slices (PCLS) derived from mouse and Human lung samples³³. PCLS have the major advantage to include the lung primary cell populations in a 3-dimensional preserved lung architecture and microenvironment. Our *Prrx1* ASO was designed to target both Human *PRRX1* and mouse *Prrx1* TFs orthologs. In basal condition, *Prrx1* knock down was associated with a decrease in *Acta2* mRNA expression only in mouse PCLS (supplemental Figure S12). Next, mouse or Human control lung PCLS were treated with a fibrosis cocktail (FC) consisting of TGF- β 1, PDGF-AB, TNF α and LPA to trigger fibrosis-like changes³³. In both mouse and Human PCLS, *ACTA2*, *A1COL1* and *FN1* mRNA upregulation was lessened in FC stimulated PCLS with *PRRX1* ASO compared to control (Figure 9A-C). We confirmed those findings at the protein levels for ACTA2 and COL1 by western blot in mouse PCLS model treated with FC in presence of *Prrx1* ASO (Figure 9B). In Human PCLS stimulated with FC, morphological analysis revealed that *PRRX1* ASO treatment was associated with decreased Collagen accumulation compared to control ASO (Figure 9D).

Altogether, these results demonstrate that inhibition of PRRX1 transcription factors, using an ASO approach, reduced fibrosis development in vivo and ex vivo.

DISCUSSION:

This is the first study to evidence the critical role of the PRRX1 transcription factors in IPF pathophysiology. Our results demonstrate that 1) PRRX1 TFs are upregulated in mesenchymal cells accumulating in the fibrotic areas of IPF lungs, 2) the expression of PRRX1 TFs is positively regulated by cues associated with an undifferentiated phenotype in control and IPF primary lung fibroblasts, 3) PRRX1 TFs are required for proliferation as well as proper myofibroblastic differentiation *in vitro* (see Figure 10 for summary). We identified the underlying mechanisms; including PRRX1 TFs effects on cell cycle (modulation of cyclins and MKI67) and on SMAD 2/3 phosphorylation (regulation of TGFBR2 and phosphatase PPM1A) respectively (see Figure 10). Finally, inhibition of *Prrx1* with LNA-modified ASO strongly impacted lung fibrosis development in *in vivo* and *ex vivo* preclinical models. Altogether, this study identifies the PRRX1 transcription factors as central to the pathophysiology of lung fibrosis, suggesting that the transcriptional activity of PRRX1 TFs might be a new therapeutic target in IPF.

Reactivation of the developmental and mesenchyme-associated PRRX1 transcription factors in IPF.

The *Prrx1* gene encodes transcription factor isoforms (*Prrx1a* and *1b*) involved in the maintenance of cell fate within the limb and craniofacial mesenchyme during ontogeny⁵. *Prrx1* is also required for cell fate decision during lung development. *Prrx1*^{-/-} newborn display hypoplastic lungs and die at birth from respiratory distress⁶. PRRX1 TFs were also identified as key drivers of mesenchymal phenotype acquisition during epithelial-mesenchyme transition (EMT) in cancer⁹.

However, the role of PRRX1 TFs in IPF, a disease associated with major perturbations in mesenchymal compartment was not known. We first identified *PRRX1* as potentially upregulated TF in IPF lung after analysis of public transcriptomic database comparing control and IPF lungs³⁴⁻³⁶. *PRRX1* also appeared in the upregulated gene hit list of a subgroup of IPF patients, displaying an accelerated clinical course in another transcriptomic study¹⁸. We confirmed that the mRNA levels of *PRRX1* TFs isoforms were actually increased in IPF lung patients as well as in primary fibroblast isolated from IPF lung compared to control ones. This increase was only confirmed at the protein level in IPF whole lung extracts compared to control ones. The upregulation of PRRX1 protein levels in fibrotic lungs may therefore reflect the accumulation of PRRX1 positive cells in IPF. Indeed, PRRX1 expression was restricted in control lungs to interstitial fibroblasts within peri-vascular and peri- bronchiolar space, while no PRRX1 signal was detected in alveolar and bronchiolar epithelia or smooth muscle cells. In IPF lungs, PRRX1 was strongly detected in the nucleus of fibroblasts organized in foci and in

scattered mesenchymal cells within the remodeled / fibrotic lung areas¹⁷. Our findings are also supported by a recent single cell transcriptomic study performed in donor and fibrotic lungs¹⁹. Datamining from this study showed that *PRRX1* expression was restricted to a subpopulation of lung fibroblasts. We also confirmed *in vitro* the strong association of *PRRX1* expression with lung fibroblast lineage, compared to primary alveolar macrophages and AEC2. Altogether, our results identified *PRRX1* isoforms as transcription factors restricted to mesenchymal / fibroblast.

***PRRX1* TFs expression is increased in lung fibroblasts by cues promoting an undifferentiated state.**

Our results clearly showed that proliferative signal such as FGF2 or anti-fibrotic secreted factor such as PGE2 up-regulated *PRRX1a* and *1b* expression in both control and IPF fibroblasts. Furthermore, substrate stiffness in physiological range increased *PRRX1* isoforms expression in a PTGS2 dependent manner.

Surprisingly, *PRRX1a* and *-1b* TF mRNA expression levels in control fibroblasts were upregulated on IPF fibroblast-derived 3D ECM in a PDGFR dependent manner. Meanwhile neither PDGF-AA nor PDGF-BB upregulated *PRRX1a* or *-1b* mRNA expression in control fibroblasts when cultured either on plastic or control fibroblast-derived 3D ECM suggesting that a ligand-independent activation of PDGFR could be involved as previously reported in other cellular systems³⁷⁻³⁹. A possible off-target effect of PDGFR V inhibitor on other tyrosine kinase receptors (TKR) cannot be completely excluded. However, we used this small inhibitory molecule at the nanomolar range (10nM) to preferentially target PDGF receptors; while cKIT, another known targeted TKR, is inhibited only at a twenty fold higher concentration⁴⁰. This potential ligand-independent activation of PDGFR triggered by IPF fibroblast-derived 3D ECM remains to be further investigated and is beyond the scope of the current work.

Nevertheless, these results suggested that the ECM secreted by IPF fibroblasts also contained cues promoting the upregulation of *PRRX1* TFs expression in control fibroblasts (see Figure 10). However, *PRRX1* TF mRNA levels in IPF fibroblasts were not modulated by those cues. In conclusion, *PRRX1* TF mRNA levels seemed to be regulated by both ECM origin and stiffness in control fibroblasts, while it was only modulated by the latter in IPF fibroblasts.

On the other hand, signals triggering myofibroblastic differentiation (TGF- β 1 stimulation and stiff substrate) decreased *PRRX1* TFs levels in primary lung fibroblasts (Figure 10). Interestingly, several studies reported that *PRRX1* expression level was rather increased upon the activation of the TGF- β pathway in other cell types such as mouse embryonic lung mesenchymal cells⁴¹, embryonic mouse 3T3-L1 adipocyte precursor⁸ and transformed epithelial cells undergoing EMT⁹. *PRRX1* upregulation in response to TGF- β 1 in the two later

cell types promoted their dedifferentiation toward a more plastic phenotype^{8,9}. Conversely, *PRRX1* downregulation in primary lung fibroblasts grown in presence of TGF- β 1 was associated with a differentiation process toward myofibroblastic phenotype.

Overall, these different studies and our results strongly suggested that *PRRX1* expression is associated with an undifferentiated phenotype in a cell and context-dependent manner.

***PRRX1* TFs drive key basic fibroblast functions involved in fibrogenesis.**

In adult lung fibroblasts, *PRRX1* TFs appeared to strongly influence cell cycle progression and myofibroblastic differentiation, two entangled cellular processes (Figure 10). There was generally no difference between control and IPF fibroblasts regarding *PRRX1* functions in those cells (with respect to proliferation and myofibroblastic differentiation at least). Overall, this may suggest that *PRRX1* TFs function might be central to fibroblast biology independently of their origin (control versus IPF lungs). However, differential *PRRX1* regulation between control and IPF fibroblasts by the micro-environment or soluble factors could therefore have a higher impact on *PRRX1* overall function in lung fibroblasts.

With respect to cell cycle progression, the G1/S arrest cell in *PRRX1* siRNA treated lung fibroblasts (Figure 10) was associated with a strong decrease of Cyclins mRNA levels involved in the replicative S phase: *Cyclin A2 (CCNA2)* and *Cyclin E2 (CCNE2)*²⁷. Furthermore, this G1/S cell cycle arrest was associated with a decrease in MKI67 positive cells suggestive of a G0 phase entry of these cells^{27,28}. The downregulation of *MKI67* expression was also observed at the mRNA level in both control and IPF fibroblasts treated with *PRRX1* siRNA. Chromatin immunoprecipitation performed in control primary NHLF demonstrated *PRRX1* binding in *CCNA2*, *CCNE2* as well as *MKI67* promoter regions suggesting that those genes could be direct *PRRX1* TFs target genes.

Meanwhile, *PRRX1* partial loss of function perturbed only some key features of myofibroblastic differentiation in response to TGF- β 1 stimulation (see Figure 10). Only the expression of markers involved in the acquisition of contractile properties (*ACTA2* and *ACTG2*) was dampened in a SMAD2/3 dependent way. The effect of *PRRX1* inhibition upon P-SMAD3 was partially mediated through TGFBR2 downregulation and the upregulation of the PPM1A phosphatase³⁰. Whole transcriptome profiling data performed in NHLF were also consistent with a global impact of *PRRX1* downregulation on TGF- β 1 response in lung fibroblasts.

Since *PRRX1* TFs binding to PPM1A promoter region was demonstrated by ChIP, this may suggest that *PPM1A* expression inhibition by *PRRX1* TFs could be direct. Indeed, *PRRX1* TFs may act as transcriptional activators or inhibitors in a context and cell -dependent manner⁴. The effect of *PRRX1* TFs upon *ACTA2* loci could be also direct since *PRRX1* binding to *ACTA2* regulatory sequences was demonstrated in NHLF by ChIP. The recruitment of *PRRX1*

TFs at the *ACTA2* loci at the level of an SRF response element (CArG boxes) was previously reported in vascular smooth muscle stimulated with Angiotensin II ²⁹.

Meanwhile, the expression levels of key ECM proteins such as Collagen 1 and Fibronectin were still upregulated in TGF- β 1 stimulated lung fibroblasts, transfected with *PRRX1* siRNA. Even though, SMAD3 phosphorylation was impacted, the non-canonical ERK, AKT and JNK pathways were still fully activated in those stimulated cells. The activation of those pathways has been previously showed to be sufficient to upregulate the expression of FN1 and Collagen in fibroblasts ^{2,30}. However, the expression of other IPF-associated ECM proteins such as TNC and ELN was perturbed in *PRRX1* siRNA treated control and IPF lung fibroblasts stimulated with TGF- β 1. Our results suggest that *PRRX1* inhibition in presence of TGF- β 1 might promote a different myofibroblastic phenotype with potentially less contractile capability and with a different ECM secretome. Albeit we showed that *PRRX1* is required for proper myofibroblastic differentiation, the expression of both *PRRX1* isoforms was decreased after TGF- β 1 treatment for 48h. This paradoxical downregulation of *PRRX1* in response to TGF- β 1, could be the signature of a negative feedback loop to limit cell-responsiveness to TGF- β 1 long exposure (Figure 10). TGF- β 1 induced *PRRX1* inhibition in lung fibroblasts could also correlate with progressive proliferation loss during differentiation process.

Overall, we propose that *PRRX1* TFs would maintain lung mesenchymal cells in an undifferentiated and proliferative state but would also act as enablers to promote full myofibroblastic differentiation in response to pro-fibrotic cues such as TGF- β 1.

Recently, Yeo *et al.* demonstrated that *PRRX1* TFs were involved in a loop in which *TWIST1* TF directly increased *PRRX1* levels which subsequently induced *TNC* that itself stimulated *TWIST1* activity. This positive feedback loop would therefore continuously activate fibroblasts ¹⁷. In this study, shRNA mediated *PRRX1* loss of function was sufficient to dampen *TNC* expression level. In our hand, *PRRX1* loss of functions in control and IPF lung fibroblasts failed to modulate to *TNC* and *TWIST1* mRNA in absence of TGF- β 1. Surprisingly, *TNC* mRNA level was even upregulated in *PRRX1* siRNA treated fibroblasts in presence of TGF- β 1. Differences in the fibroblast origin may explain this discrepancy: fetal Human lung fibroblasts (IMR90 and MRC5) or CAFs in the work of Yeo *et al.* ¹⁷, while we were using primary fibroblasts derived from control and IPF adult lungs. Similarly, the upregulation of *TNC* downstream of *PRRX1* TFs was first unveiled in mouse fibroblasts of embryonic origin ⁴². Altogether, those studies and ours strongly suggest that *PRRX1* TFs function might be context and even age - dependent within cells of mesenchymal origins.

Inhibition of the mesenchymal *PRRX1* transcription factor is sufficient to dampen lung fibrosis *in vivo*.

PRRX1 TFs expression levels were also upregulated during the fibrosis phase at day 14 in mice treated with bleomycin (intratracheal route).

However, the *Prrx1* homozygous and heterozygous mice were not suitable for studying *Prrx1* function during lung fibrosis in adult mice. Indeed, *Prrx1*^{-/-} mice present a lethal respiratory failure at birth^{5,6,32} and the lack of haploinsufficiency in *Prrx1*^{+/-} heterozygous mice did not prevent lung fibrosis development after intratracheal instillation of bleomycin. Thus, we chose to inhibit *Prrx1* in adult mice using a LNA-modified ASO⁴³ targeting both *Prrx1* isoforms. This ASO was administered by the endotracheal route in a “curative” protocol from day 7 in this experimental mouse model of pulmonary fibrosis. LNA-modified ASOs are protected from nuclease-mediated degradation, which significantly improves their stability and prolongs their activity *in vivo*. In comparison to earlier generations of ASO modifications, they have a massively increased affinity to their target RNA and their *in vitro* and *in vivo* activity does not depend on delivery reagents⁴³. As a proof of concept, we confirmed that intratracheal administration of *Prrx1*-specific ASO inhibited the upregulation of mouse PRRX1a and -1b expression at both mRNA and protein level at day 14 in bleomycin treated mice. Pulmonary fibrosis development was also reduced in these animals. While our *in vitro* findings in adult Human lung fibroblasts showed that PRRX1 inhibition mainly impacted ACTA2 expression levels, *Prrx1* ASO treatment in the bleomycin mouse model of lung fibrosis also inhibited the deposition of Collagen and Fibronectin. This difference regarding ECM compound at day 14 may reflect the effect of *Prrx1* ASO on the overall fibrosis development; upon the proliferation / accumulation as well as impaired myofibroblastic differentiation of mesenchymal cells *in vivo* from the beginning of the ASO treatment at day 7. We confirmed the anti-fibrotic effect of the *Prrx1* ASO in a second model of fibrosis using *ex vivo* culture of Human or mouse PCLS stimulated with a cocktail of fibrosis-associated cytokines³³.

Targeting of others transcription factors such as GLI³¹, FOXM1⁴⁴, FOXF1⁴⁵, FOXO3⁴⁶ and TBX4⁴⁷ was also shown to inhibit fibrosis development in this mouse experimental model of pulmonary fibrosis. However, at the exception of TBX4 and PRRX1, the expression of all these other TFs is not restricted to mesenchymal lineages, which means that targeting those TFs may impact both lung fibrosis and epithelial regeneration/repair. Finally, PRRX1 inhibition as a potential therapeutic approach in fibrosis is not restricted to the lung. Recently, adenoviral shRNA mediated inhibition of *Prrx1* in the thioacetamide model of liver fibrosis in rats also decreased fibrotic lesions, collagen deposition and hepatic stellate cells myofibroblastic differentiation¹².

In conclusion, our study unveils the role of the pro-fibrotic and mesenchyme associated PRRX1 TFs in lung fibrosis. Direct inhibition of PRRX1 transcriptional activity in mesenchymal cells may be a potential therapeutic target in IPF. Furthermore, the effectiveness of the late administration of *Prrx1* ASO in the bleomycin model of pulmonary fibrosis is particularly

interesting. The route of administration we used constitutes a first attempt to locally inhibit a pro-fibrotic TF. The possibility of a local administration of an antifibrotic is seductive: current antifibrotics, administered systemically, are burdened with significant adverse events, which significantly attenuates their effect on health-related quality of life ⁴⁸. Inhaled pirfenidone and other inhaled compounds ⁴⁹ are currently investigated in IPF, but none are directly acting on a mesenchymal transcription factor. Although already proved effective in asthma ⁵⁰, local transcription factor inhibition has never been investigated in IPF so far.

METHODS:

Human lung samples.

IPF lung samples were obtained from patients undergoing open lung biopsy or at the time of lung transplantation ($n = 39$; median age 61 yr; range 51–70 yr). IPF was diagnosed according to 2011 ATS/ERS/JRS/ALAT criteria, including histopathological features of usual interstitial pneumonia⁵¹. Lung samples obtained after cancer surgery, away from the tumor, were used as controls; normalcy of control lungs was verified histologically ($n = 35$ patients; median age 64 yr, range 28–83 yr).

In vivo experiments.

All experiments were performed using adult male C57BL/6 mice and intratracheal bleomycin administration, as previously described³¹. To investigate the involvement of PRRX1 in fibrogenesis, mice were treated with third generation locked nucleic acid (LNA)-modified ASO targeting PRRX1 designed by Secarna Pharmaceuticals GmbH & Co, Planegg/Martinsried, Germany. The following sequence was used (+ indicates an LNA modification, while * indicates a phosphorothioate (PTO) linkage) to target *Prrx1* (*Prrx1* ASO):
+T*C*+A*+G*G*T*T*G*G*C*A*A*T*G*+C*+T*+G

A previously published and validated⁵² negative control ASO (Cont ASO) was used:

+C*+G*+T*T*T*A*G*G*C*T*A*T*G*T*A*+C*+T*+T

Bleomycin control mice received only PBS. ASO and PBS were given by endotracheal instillation every other day from Day 7 after the bleomycin injection, until Day 13. All the mice were under isoflurane anesthesia during the instillation and received one injection every other day of 25 μ L with 20nmol of ASO or PBS1X. Lungs were harvested on Day 14 for further analysis. Hematoxylin, eosin and picosirius staining were performed routinely to evaluate the morphology of the lung. Semiquantitative histological assessment of lung injury used the grading system described by Inoshima and colleagues⁵³. Total mRNA was extracted from mouse lung homogenates, and the expression of the genes of interest was quantified by real-time PCR, as previously described. Proteins were extracted from mouse lung homogenates and western blotting was performed by standard techniques as previously described³¹.

The *Prrx1* heterozygous mouse strain (129S-*Prrx1*^{tm1Jfm}/Mmmh³², RRID:MMRRC_000347-MU) was obtained from the Mutant Mouse Resource and Research Center (MMRRC) at University of Missouri (USA), an NIH-funded strain repository, and was donated to the MMRRC by Pr James Martin (Texas Agricultural and Mechanical University: Health Science Center, USA).

Statistical Analysis.

Most data are represented as dot plots with median, unless specified. All statistical analysis were performed using Prism 5 (GraphPad Software, La Jolla, CA). We used non-parametric Mann-Whitney U test for comparison between two experimental conditions. Paired data were compared with Wilcoxon signed-rank test. We used non-parametric Kruskal Wallis test followed by Dunn's comparison test for group analysis. Comparison of histological scores on Day 14 was performed with Fisher's exact test. A p-value < 0.05 was considered to be statistically significant. Exact *P* values and definition and number of replicates are given in the respective figure legend.

Study approval.

The study on human material was performed in accordance with the Declaration of Helsinki and approved by the local ethics committee (CPP Ile de France 1, No.0811760). Written informed consent was obtained from all subjects.

All animal experiments were conducted in accordance with the Directive 2010/63/EU of the European Parliament and approved by the local Animal ethics committee ("Comité d'éthique Paris Nord n°121", APAFiS #4778 Etudedufacteurdetran_2016031617411315).

See supplementary materials for further details.

Author contributions:

EMD, MHL, AF, MJ, EF, MG, AJ, AM, AJ, AAM, LG, AV, MK, CMM carried out the experiments; KS and FJ designed and provided reagents; AC, HM, PM provided the lung samples; AAM, BC supervised the study. AAM, BC, MHL, AF, CMM, AG, BM and EMD designed the work, analyzed the data and wrote the manuscript. All authors reviewed and approved the manuscript.

Acknowledgements:

We thank Olivier Thibaudeau and Laure Wingertsmann (Morphology Platform, Inserm U1152 of X. Bichat Medical School, Paris) for their efficient collaboration and the Flow Cytometry Platform of Inserm U1149 (CRI, X. Bichat Medical School, Paris) as well. We also thank Dr. J.W. Duitman (Academic Medical Center, Amsterdam, The Netherlands) for his technical help. This work was supported by the ANR (JCJC ANR-16-CE14-0018), by grants from the Chancellery of Paris Universities (Poix Legacy), and by the “Association pour la fibrose pulmonaire idiopathique Pierre ENJALRAN”. E. Marchal-Duval was supported by “Ecole Doctorale Bio-SPC” (Grant 2015) ; A. Froidure an European Respiratory Society (ERS) and the European Molecular Biology Organization (EMBO) - ERS-LTRF 2015 – 4476 and by a fellowship from the Belgian Society for Pulmonology (BVP-SBP); M Homps-Legrand by the Fond de dotation “Recherche en Santé Respiratoire” (Grant 2018). A. Justet by the “Fondation Recherche Médicale” (Grant FRM 2016, FDM41320); M. Ghanem by the Fond de dotation “Recherche en Santé Respiratoire” (Grant 2015) and A Maurac by the ARS Lorraine (« année Recherche » 2016). We thank Alberto Baeri (IPMC), Nicolas Nottet (C3M, Nice) and Kevin Lebrigand (UCA genomics platform, IPMC) for their technical help. The authors declare no conflicts of interest.

REFERENCES:

1. Martinez, F. J. *et al.* Idiopathic pulmonary fibrosis. *Nat. Rev. Dis. Primer* **3**, 17074 (2017).
2. Fernandez, I. E. & Eickelberg, O. New cellular and molecular mechanisms of lung injury and fibrosis in idiopathic pulmonary fibrosis. *Lancet Lond. Engl.* **380**, 680–688 (2012).
3. Selman, M., Pardo, A. & Kaminski, N. Idiopathic pulmonary fibrosis: aberrant recapitulation of developmental programs? *PLoS Med.* **5**, e62 (2008).
4. Norris, R. A. & Kern, M. J. The identification of Prx1 transcription regulatory domains provides a mechanism for unequal compensation by the Prx1 and Prx2 loci. *J. Biol. Chem.* **276**, 26829–26837 (2001).
5. Martin, J. F., Bradley, A. & Olson, E. N. The paired-like homeo box gene M_{Hox} is required for early events of skeletogenesis in multiple lineages. *Genes Dev.* **9**, 1237–1249 (1995).
6. Ihida-Stansbury, K. *et al.* Paired-related homeobox gene Prx1 is required for pulmonary vascular development. *Circ. Res.* **94**, 1507–1514 (2004).
7. Shimosaki, K., Clemenson, G. D. & Gage, F. H. Paired related homeobox protein 1 is a regulator of stemness in adult neural stem/progenitor cells. *J. Neurosci. Off. J. Soc. Neurosci.* **33**, 4066–4075 (2013).
8. Du, B. *et al.* The transcription factor paired-related homeobox 1 (Prrx1) inhibits adipogenesis by activating transforming growth factor- β (TGF β) signaling. *J. Biol. Chem.* **288**, 3036–3047 (2013).
9. Ocaña, O. H. *et al.* Metastatic colonization requires the repression of the epithelial-mesenchymal transition inducer Prrx1. *Cancer Cell* **22**, 709–724 (2012).
10. Fazilaty, H. *et al.* A gene regulatory network to control EMT programs in development and disease. *Nat. Commun.* **10**, 5115 (2019).
11. Reichert, M. *et al.* The Prrx1 homeodomain transcription factor plays a central role in pancreatic regeneration and carcinogenesis. *Genes Dev.* **27**, 288–300 (2013).
12. Gong, J. *et al.* Paired related homeobox protein 1 regulates PDGF-induced chemotaxis of hepatic stellate cells in liver fibrosis. *Lab. Investig. J. Tech. Methods Pathol.* **97**, 1020–1032 (2017).
13. Tomaru, Y. *et al.* A transient disruption of fibroblastic transcriptional regulatory network facilitates trans-differentiation. *Nucleic Acids Res.* **42**, 8905–8913 (2014).
14. Leavitt, T. *et al.* Prrx1 Fibroblasts Represent a Pro-fibrotic Lineage in the Mouse Ventral Dermis. *Cell Rep.* **33**, 108356 (2020).
15. Currie, J. D. *et al.* The Prrx1 limb enhancer marks an adult subpopulation of injury-responsive dermal fibroblasts. *Biol. Open* **8**, (2019).
16. Xie, T. *et al.* Single-Cell Deconvolution of Fibroblast Heterogeneity in Mouse Pulmonary Fibrosis. *Cell Rep.* **22**, 3625–3640 (2018).
17. Yeo, S.-Y. *et al.* A positive feedback loop bi-stably activates fibroblasts. *Nat. Commun.* **9**, 3016 (2018).
18. Selman, M. *et al.* Accelerated variant of idiopathic pulmonary fibrosis: clinical behavior and gene expression pattern. *PloS One* **2**, e482 (2007).
19. Reyfman, P. A. *et al.* Single-Cell Transcriptomic Analysis of Human Lung Provides Insights into the Pathobiology of Pulmonary Fibrosis. *Am. J. Respir. Crit. Care Med.* (2018) doi:10.1164/rccm.201712-2410OC.
20. Adams, T. S. *et al.* Single-cell RNA-seq reveals ectopic and aberrant lung-resident cell populations in idiopathic pulmonary fibrosis. *Sci. Adv.* **6**, eaba1983 (2020).

21. Bonner, J. C. Regulation of PDGF and its receptors in fibrotic diseases. *Cytokine Growth Factor Rev.* **15**, 255–273 (2004).
22. Booth, A. J. *et al.* Acellular normal and fibrotic human lung matrices as a culture system for in vitro investigation. *Am. J. Respir. Crit. Care Med.* **186**, 866–876 (2012).
23. Liu, F. *et al.* Feedback amplification of fibrosis through matrix stiffening and COX-2 suppression. *J. Cell Biol.* **190**, 693–706 (2010).
24. Zhou, Y. *et al.* Inhibition of mechanosensitive signaling in myofibroblasts ameliorates experimental pulmonary fibrosis. *J. Clin. Invest.* **123**, 1096–1108 (2013).
25. Castelló-Cros, R. & Cukierman, E. Stromagenesis during tumorigenesis: characterization of tumor-associated fibroblasts and stroma-derived 3D matrices. *Methods Mol. Biol. Clifton NJ* **522**, 275–305 (2009).
26. Grimminger, F., Günther, A. & Vancheri, C. The role of tyrosine kinases in the pathogenesis of idiopathic pulmonary fibrosis. *Eur. Respir. J.* **45**, 1426–1433 (2015).
27. Lim, S. & Kaldis, P. Cdks, cyclins and CKIs: roles beyond cell cycle regulation. *Dev. Camb. Engl.* **140**, 3079–3093 (2013).
28. Sobocki, M. *et al.* Cell-Cycle Regulation Accounts for Variability in Ki-67 Expression Levels. *Cancer Res.* **77**, 2722–2734 (2017).
29. Hautmann, M. B., Thompson, M. M., Swartz, E. A., Olson, E. N. & Owens, G. K. Angiotensin II-induced stimulation of smooth muscle alpha-actin expression by serum response factor and the homeodomain transcription factor MHOX. *Circ. Res.* **81**, 600–610 (1997).
30. Bruce, D. L. & Sapkota, G. P. Phosphatases in SMAD regulation. *FEBS Lett.* **586**, 1897–1905 (2012).
31. Moshai, E. F. *et al.* Targeting the hedgehog-glioma-associated oncogene homolog pathway inhibits bleomycin-induced lung fibrosis in mice. *Am. J. Respir. Cell Mol. Biol.* **51**, 11–25 (2014).
32. Lu, M. F. *et al.* prx-1 functions cooperatively with another paired-related homeobox gene, prx-2, to maintain cell fates within the craniofacial mesenchyme. *Dev. Camb. Engl.* **126**, 495–504 (1999).
33. Lehmann, M. *et al.* Differential effects of Nintedanib and Pirfenidone on lung alveolar epithelial cell function in ex vivo murine and human lung tissue cultures of pulmonary fibrosis. *Respir. Res.* **19**, 175 (2018).
34. Cho, J.-H. *et al.* Systems biology of interstitial lung diseases: integration of mRNA and microRNA expression changes. *BMC Med. Genomics* **4**, 8 (2011).
35. Meltzer, E. B. *et al.* Bayesian probit regression model for the diagnosis of pulmonary fibrosis: proof-of-principle. *BMC Med. Genomics* **4**, 70 (2011).
36. Wang, X. M. *et al.* Caveolin-1: a critical regulator of lung fibrosis in idiopathic pulmonary fibrosis. *J. Exp. Med.* **203**, 2895–2906 (2006).
37. Dalvi, P. N., Gupta, V. G., Griffin, B. R., O'Brien-Ladner, A. & Dhillon, N. K. Ligand-Independent Activation of Platelet-Derived Growth Factor Receptor β during Human Immunodeficiency Virus-Transactivator of Transcription and Cocaine-Mediated Smooth Muscle Hyperplasia. *Am. J. Respir. Cell Mol. Biol.* **53**, 336–345 (2015).
38. Saito, S. *et al.* Ligand-independent trans-activation of the platelet-derived growth factor receptor by reactive oxygen species requires protein kinase C-delta and c-Src. *J. Biol. Chem.* **277**, 44695–44700 (2002).
39. Herrlich, A. *et al.* Ligand-independent activation of platelet-derived growth factor receptor is a necessary intermediate in lysophosphatidic, acid-stimulated mitogenic activity in L cells. *Proc. Natl. Acad. Sci. U. S. A.* **95**, 8985–8990 (1998).

40. Furuta, T. *et al.* Identification of potent and selective inhibitors of PDGF receptor autophosphorylation. *J. Med. Chem.* **49**, 2186–2192 (2006).
41. Li, A. *et al.* Mesodermal ALK5 controls lung myofibroblast versus lipofibroblast cell fate. *BMC Biol.* **14**, 19 (2016).
42. McKean, D. M. *et al.* FAK induces expression of Prx1 to promote tenascin-C-dependent fibroblast migration. *J. Cell Biol.* **161**, 393–402 (2003).
43. Soifer, H. S. *et al.* Silencing of gene expression by gymnotic delivery of antisense oligonucleotides. *Methods Mol. Biol. Clifton NJ* **815**, 333–346 (2012).
44. Penke, L. R. *et al.* FOXM1 is a critical driver of lung fibroblast activation and fibrogenesis. *J. Clin. Invest.* **128**, 2389–2405 (2018).
45. Black, M. *et al.* FOXF1 Inhibits Pulmonary Fibrosis by Preventing CDH2-CDH11 Cadherin Switch in Myofibroblasts. *Cell Rep.* **23**, 442–458 (2018).
46. Al-Tamari, H. M. *et al.* FoxO3 an important player in fibrogenesis and therapeutic target for idiopathic pulmonary fibrosis. *EMBO Mol. Med.* **10**, 276–293 (2018).
47. Xie, T. *et al.* Transcription factor TBX4 regulates myofibroblast accumulation and lung fibrosis. *J. Clin. Invest.* **126**, 3063–3079 (2016).
48. Graney, B. A. & Lee, J. S. Impact of novel antifibrotic therapy on patient outcomes in idiopathic pulmonary fibrosis: patient selection and perspectives. *Patient Relat. Outcome Meas.* **9**, 321–328 (2018).
49. Kaminskas, L. M. *et al.* Aerosol Pirfenidone Pharmacokinetics after Inhaled Delivery in Sheep: a Viable Approach to Treating Idiopathic Pulmonary Fibrosis. *Pharm. Res.* **37**, 3 (2019).
50. Krug, N. *et al.* Allergen-induced asthmatic responses modified by a GATA3-specific DNase. *N. Engl. J. Med.* **372**, 1987–1995 (2015).
51. Raghu, G. *et al.* An official ATS/ERS/JRS/ALAT statement: idiopathic pulmonary fibrosis: evidence-based guidelines for diagnosis and management. *Am J Respir Crit Care Med* **183**, 788–824 (2011).
52. Jaschinski, F., Korhonen, H. & Janicot, M. Design and Selection of Antisense Oligonucleotides Targeting Transforming Growth Factor Beta (TGF- β) Isoform mRNAs for the Treatment of Solid Tumors. *Methods Mol. Biol. Clifton NJ* **1317**, 137–151 (2015).
53. Inoshima, I. *et al.* Anti-monocyte chemoattractant protein-1 gene therapy attenuates pulmonary fibrosis in mice. *Am. J. Physiol. Lung Cell. Mol. Physiol.* **286**, L1038-1044 (2004).

FIGURES:

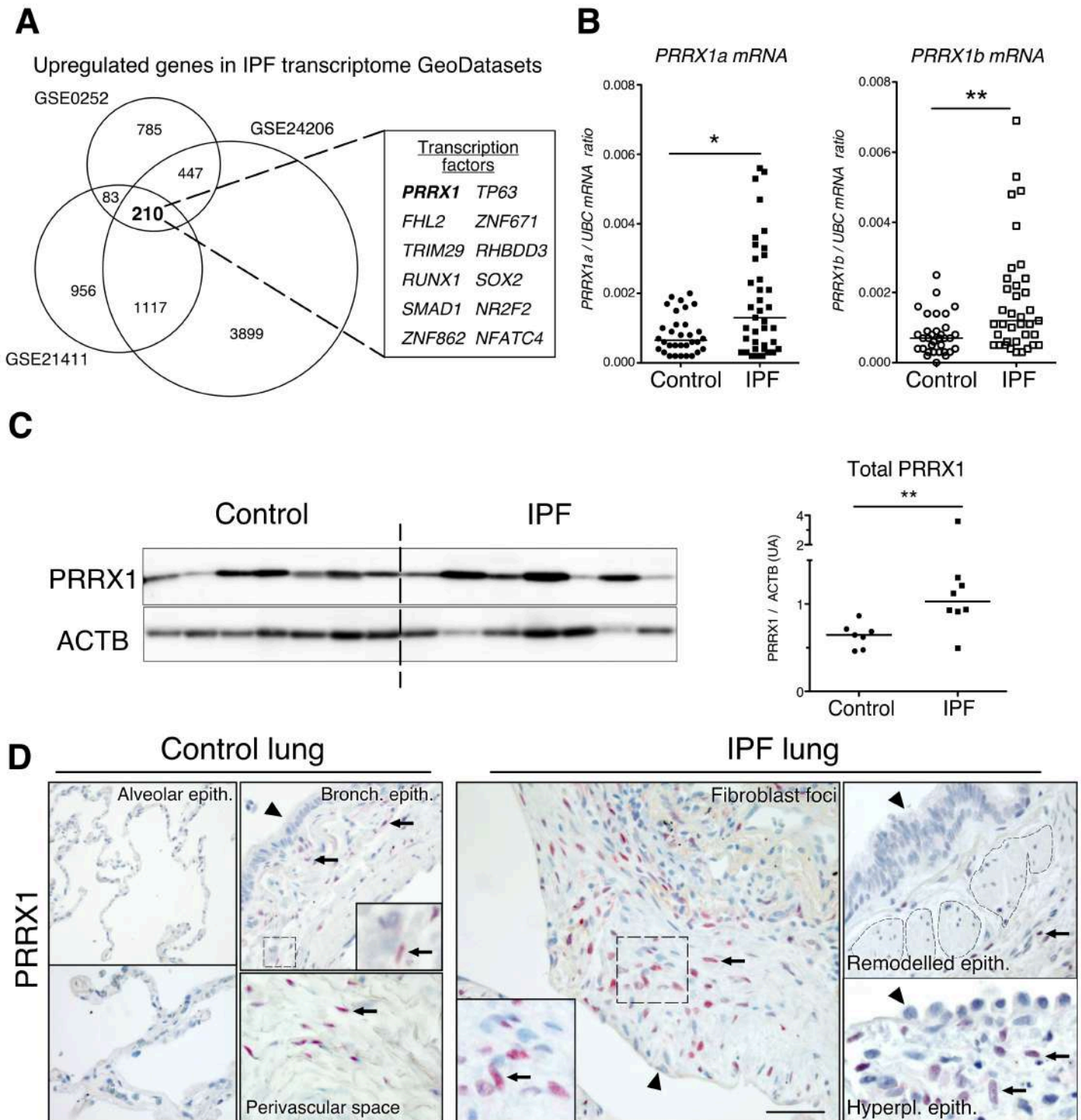


Figure 1

Figure 1: Identification of PRRX1 as a transcription factor reactivated in IPF lung.

(A) Venn diagram showing the number of genes up-regulated in three IPF lung Transcript microarray databases compared to controls (NCBI GEO GDS1252, GDS4279, GDS3951). Among the 210 common upregulated genes in all three datasets, 12 genes were annotated as transcription factors (table, PRRX1 is in bold). (B) Dot plots with median showing the mRNA expression of *PRRX1a* and *PRRX1b* isoforms in control (circle, n=35) and IPF (square, n=38) whole lung homogenates. (C) Immunoblot showing PRRX1 expression in control and IPF whole lung homogenates. ACTB was used as loading control. The quantification of PRRX1 relative expression to ACTB in control (circle, n=7) and IPF (square, n=8) is displayed as dot plot with median on the right. (D) Representative immunohistochemistry images (n=5 per group) showing PRRX1 staining (red) in control (left panels) and IPF (right panels). Nuclei were counterstained with hematoxylin. Note the absence of PRRX1 staining in the alveolar and bronchiolar epithelium (arrow head). PRRX1 positive cells were only detected in the peri-bronchiolar and peri-vascular spaces (arrows) in control lungs (left panels). In IPF, PRRX1 positive cells (arrow) were detected in the remodeled/fibrotic area (right panels). Note that epithelial cells (arrow head) and bronchiolar smooth muscle cells (dashed areas) are PRRX1 negative. The high magnification pictures match the dashed boxes displayed in the main panels. (Scale bar: 80µm in low magnification images and 25µm in high magnification ones) (Abbreviations: *epithelium. (epith)*; *bronchiolar. (bronch)*; *Hyperpl. (hyperplastic)*). Mann Whitney U test, *p≤0.05, **p≤0.01.

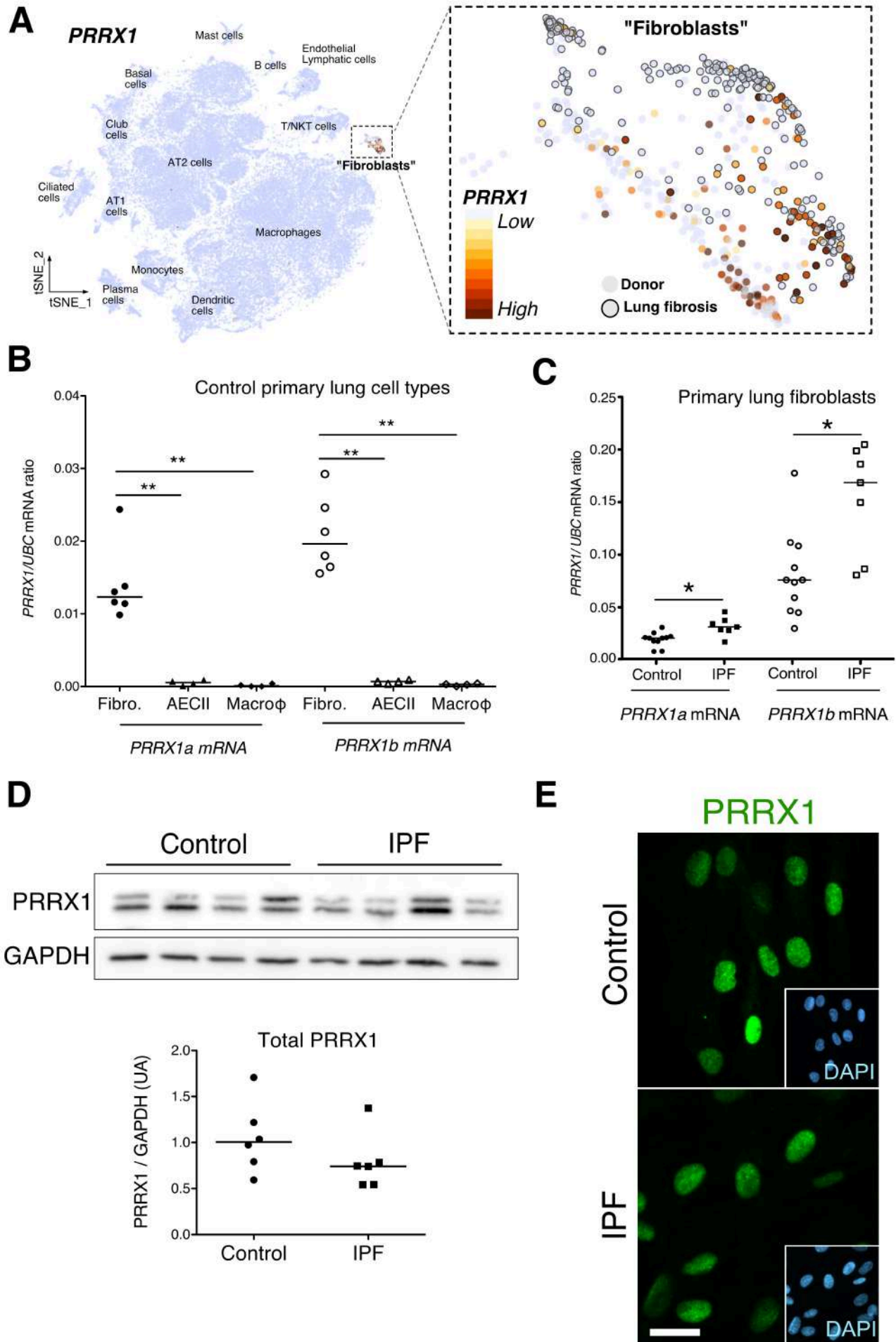


Figure 2

Figure 2: PRRX1 is a mesenchymal transcription factor upregulated in primary Human lung IPF fibroblasts.

(A) Integrated single-cell RNA-Seq analysis of donors as well as patients with pulmonary fibrosis showing diverse lung cell populations using previously published data from ¹⁹ (source: www.nupulmonary.org/resources/). *PRRX1* mRNA expression was used to label clusters by cell identity as represented in the tSNE plot. Note that *PRRX1* mRNA expression is restricted to cell types classified as “Fibroblasts”. (B) Dot plots with median showing the mRNA expression of *PRRX1a* (black) and *PRRX1b* (white) isoforms in primary Human lung fibroblasts (circle, n=6), alveolar epithelial cells (triangle, n=4) and alveolar macrophages (diamond, n=4). (C) Dot plots with median showing the mRNA expression of *PRRX1a* (black) and *PRRX1b* (white) isoforms in control (circle, n=11) and IPF (square, n=7) primary Human lung fibroblasts. (D) Immunoblot showing PRRX1 expression in control and IPF primary Human lung fibroblasts. GAPDH was used as loading control. The quantification of PRRX1 relative expression to GAPDH in control (circle, n=6) and IPF (square, n=6) lung fibroblasts is displayed as dot plot with median below. (E) Representative Immunofluorescence images (n=8 per group) showing PRRX1 staining (green) in control (top panel) and IPF (bottom panel) fibroblasts. Nuclei were counterstained with DAPI (inserts in main panels). (Scale bar 20µm in main panels and 40µm in inserts); (Abbreviations: fibroblasts (*fibro*); alveolar epithelial cells (*AECII*); alveolar macrophages (*macroφ*)). Mann Whitney U test, *p≤0.05.

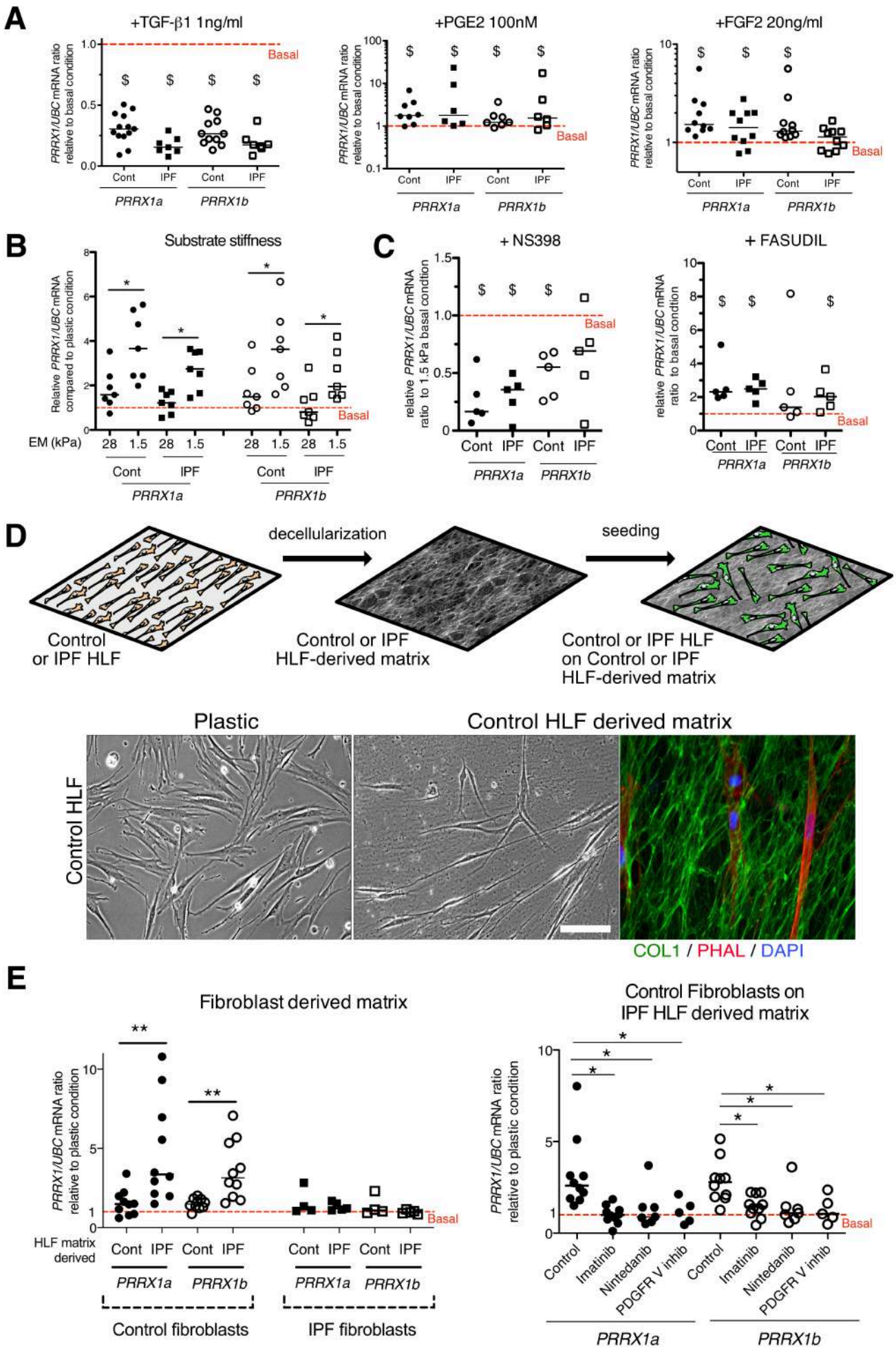


Figure 3

Figure 3: PRRX1 is modulated by growth factors and matrix environment.

(A) Dot plots with median showing the mRNA expression of *PRRX1a* (black) and *PRRX1b* (white) isoforms in control (circle) and IPF (square) primary Human lung fibroblasts stimulated for 48h with TGF- β 1 (left, n=6-7), PGE2 (middle, n=6-7) and FGF2 (right, n=10) compared to basal condition (red dashed line). (B) dot plots with median showing the mRNA expression of *PRRX1a* and *PRRX1b* isoforms in control (n=7) and IPF (n=7) lung fibroblasts cultured on stiff (28kPa) and soft (1.5kPa) substrate compared to basal condition. (C) Dot plots with median showing the mRNA expression of *PRRX1a* and *PRRX1b* isoforms in control and IPF lung fibroblasts (n=5) stimulated 48h with NS398 (left), or Fasudil (right) compared to basal condition. (D) Summary sketch of Fibroblast-derived matrix experiments (upper part). Lower part: representative phase contrast pictures of control primary lung fibroblasts on plastic (left) or seeded in a control fibroblast-derived matrix (middle) and immunofluorescence pictures (right) of Collagen 1 (green) revealing the HLF-derived matrix and actin fibers stained with Phalloidin (red). Nuclei were counterstained with DAPI (blue). (E) Left panel: dot plots with median showing the mRNA expression of *PRRX1a* and *PRRX1b* isoforms in control (n=10) or IPF fibroblasts (n=5) seeded on control or IPF derived matrix compared to basal condition. Right panel: dot plots with median showing the mRNA expression of *PRRX1a* and *PRRX1b* isoforms in control fibroblasts cultured on IPF derived matrix and stimulated with Imatinib (n=10), Nintedanib (n=7) or PDGFR V inhibitor (n=5) compared to basal condition. (Scale bar: 30 μ m in phase contrast pictures and 15 μ m in the immunofluorescence one) (*Abbreviations: Control (Cont), Human lung fibroblast (HLF), Elastic/Young modulus (EM), PHAL (Phalloidin), COL1 (Collagen 1)*). Mann Whitney U test, *p \leq 0.05 **p \leq 0.01; Wilcoxon signed-rank test \$ p \leq 0.05.

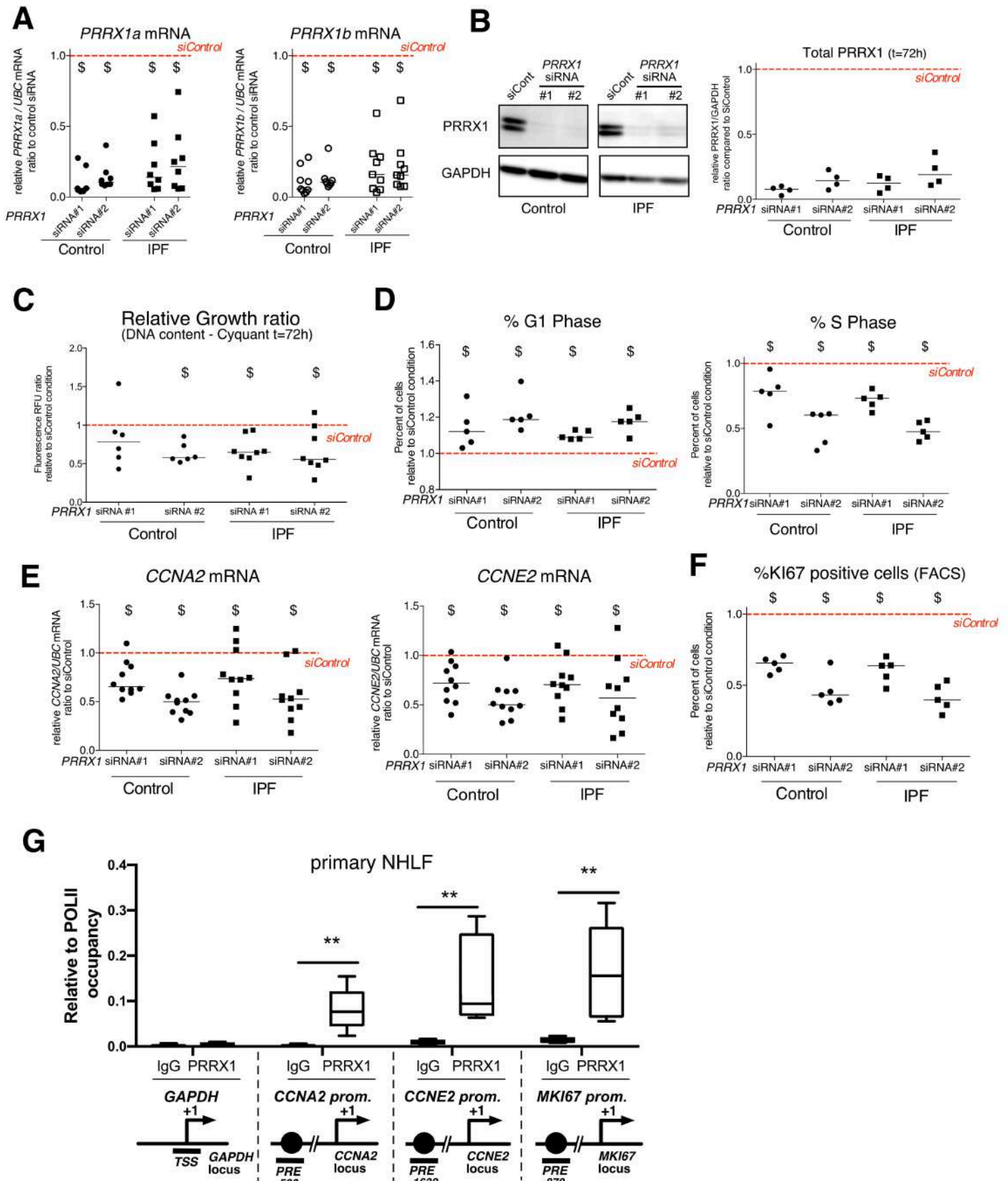


Figure 4

Figure 4: *PRRX1* knock down decreased cell proliferation.

(A) Dot plots with median showing *PRRX1a* (black) and *PRRX1b* (white) mRNA expression relative to the siControl condition (red dashed line) in control (circle) and IPF (square) fibroblasts (n=8) treated for 48h with *PRRX1* siRNA (#1 or #2). (B) Immunoblot showing *PRRX1* expression (n=4) in control and IPF fibroblasts treated 48h with *PRRX1* siRNA (#1 or #2) or siControl. The quantification of *PRRX1* expression relative to GAPDH (loading control) is displayed as dot plot with median. (C) Dot plots with median showing the relative growth ratio of control (n=6) and IPF (n=8) fibroblasts stimulated 72h with FCS 10% and treated with *PRRX1* siRNA compared to siControl. (D) Dot plots with median showing the percent of cells in G1 (right) or S (left) phase in control and IPF fibroblasts (n=5) stimulated 72h with FCS and *PRRX1* siRNA relative to siControl. (E) Dot plots with median showing mRNA expression of *CCNA2* and *CCNE2* relative to siControl in control and IPF fibroblasts stimulated 72h with FCS and treated with *PRRX1* siRNA (n=10). (F) Dot plots with median showing the percent of cells positive for Ki67 marker in control and IPF fibroblasts stimulated 72h with FCS 10% and treated with *PRRX1* siRNA relative to siControl (n=5). (G) ChIP analysis for *PRRX1* recruitment at the promoter of *GAPDH*, *CCNA2*, *CCNE2* and *MKI67* in NHLF (n=5) relative to RNA POL-II occupancy, displayed as boxes with median and min to max. The diagrams of the different loci are showing the *PRRX1* response element position relative to the TSS. The PCR amplified regions are underscored. (Abbreviations: FCS (fetal calf serum), TSS (transcription starting site); IgG (Immunoglobulin); PRE (*PRRX1* responses element); SRE (SRF response element), control siRNA sequence (siControl)). Wilcoxon signed-rank test, \$ p≤0.05, Wilcoxon matched-paired signed rank test **p<0.01.

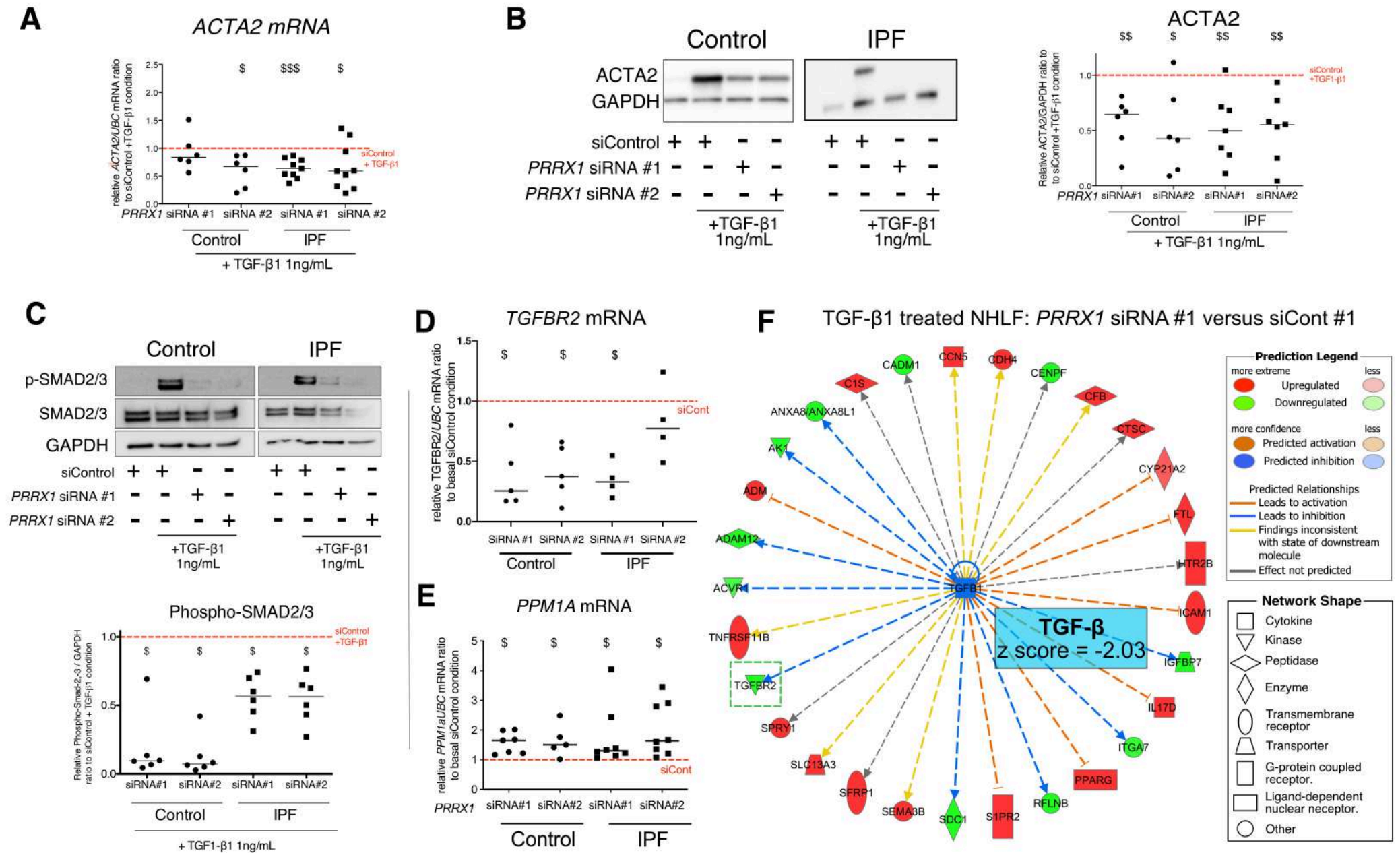


Figure 5

Figure 5: *PRRX1* inhibition decreased myofibroblast differentiation upon TGF- β 1 stimulation.

(A) Dot plots with median showing the mRNA expression of *ACTA2* relative to the siControl +TGF- β 1 condition (red dashed line), in control (circle, n=6) and IPF (square, n=9) lung fibroblasts treated with TGF- β 1 and *PRRX1* siRNA (#1 or #2). (B) Immunoblot showing *ACTA2* expression in control (n=6) and IPF (n=7) fibroblasts treated with siControl in absence or presence of TGF- β 1 or with *PRRX1* siRNA and TGF- β 1. The quantification of *ACTA2* expression relative to GAPDH (loading control) in control and IPF fibroblasts treated with control or *PRRX1* siRNA in presence of TGF- β 1 relative to siControl + TGF- β 1 condition is displayed as dot plot with median on the right. (C) Immunoblot showing phospho-SMAD2/3 and SMAD2/3 expression in control and IPF fibroblasts treated for 30 minutes with TGF- β 1 after 48h transfection with *PRRX1* siRNA. The quantification of phospho-SMAD2/3 and SMAD2/3 expression relative to GAPDH (loading control) in control (n=6) and IPF (n=6) lung fibroblasts treated for 30 minutes with TGF- β 1 after 48h transfection with *PRRX1* siRNA relative to siControl + TGF- β 1 condition (red dashed line), is displayed as dot plot with median on the right. (D-E) Dot plots with median showing the mRNA expression of *TGFBR2* (D, n=4 to 5) or *PPM1A* (E, n=7 to 8) relative to siControl in control and IPF fibroblasts treated for 48h with *PRRX1* siRNA. (F) Ingenuity Pathway Analysis of whole transcriptome in NHLF treated for 48h with *PRRX1* siRNA in the presence of TGF- β 1 indicated that the best predicted upstream regulator was TGFB1 (z score=-2.03, *PRRX1* siRNA#1 versus siControl#1, n=2). Inhibition of *TGFBR2* is framed with a green dashed border. Figure legend displays molecules and function symbol types and colors. (Abbreviations: control siRNA sequence (*siControl*), β -Tubulin (*TUB*)). Wilcoxon signed-rank test, \$ p \leq 0.05, \$\$ p \leq 0.01, \$\$\$ p \leq 0.001.

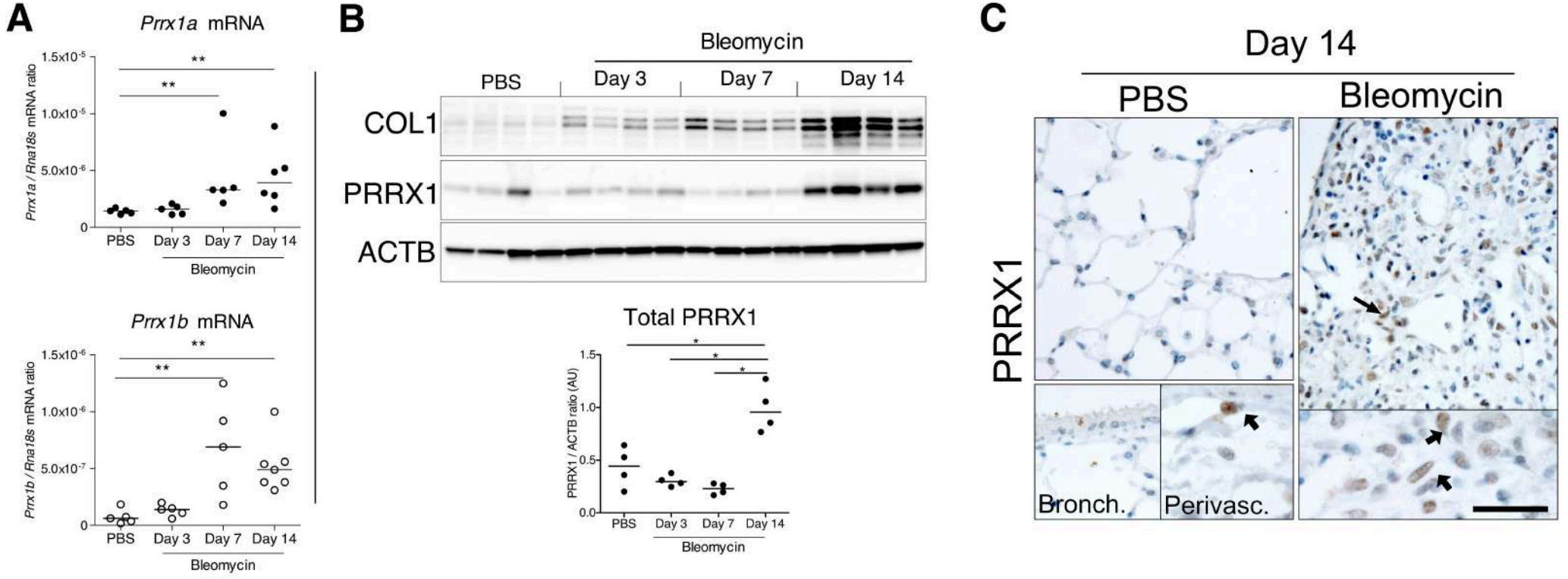


Figure 6

Figure 6: PRRX1 is increased during fibrotic phase in mice bleomycin-induced fibrosis.

(A) Dot plots with median showing the mRNA expression of *Prrx1a* (black circle) and *Prrx1b* (white circle) isoforms in PBS mice (n=5) and bleomycin-treated mice at day 3 (n=5), 7 (n=5) and 14 (n=6). (B) Immunoblot showing COL1 and PRRX1 expression in PBS and bleomycin-treated mice at day 3, 7 and 14 (n=4 per group). ACTB was used as loading control. The quantification of PRRX1 expression relative to ACTB in PBS and bleomycin mice is displayed as dot plot with median in the lower part of the panel. (C) Representative immunohistochemistry pictures (n=3 per group) showing PRRX1 staining (brown) in PBS and bleomycin mice at day 14 after saline or bleomycin administration. Nuclei were counterstained with hematoxylin. Note the absence of PRRX1 staining in the bronchiolar epithelium. PRRX1 positive cells were only detected in the peri-vascular spaces (arrows) in naive mice lungs (lower left panels). In bleomycin-treated mice, PRRX1 positive cells (arrow) were detected in the remodeled/fibrotic area (right panels). (Scale bar: 30µm in low magnification images and 15µm in high magnification ones). (Abbreviations: *bronchiolar. (bronch)*; *perivascular (perivasc)*). Kruskal-Wallis test with Dunns post-test, *p≤0.05, **p≤0.01.

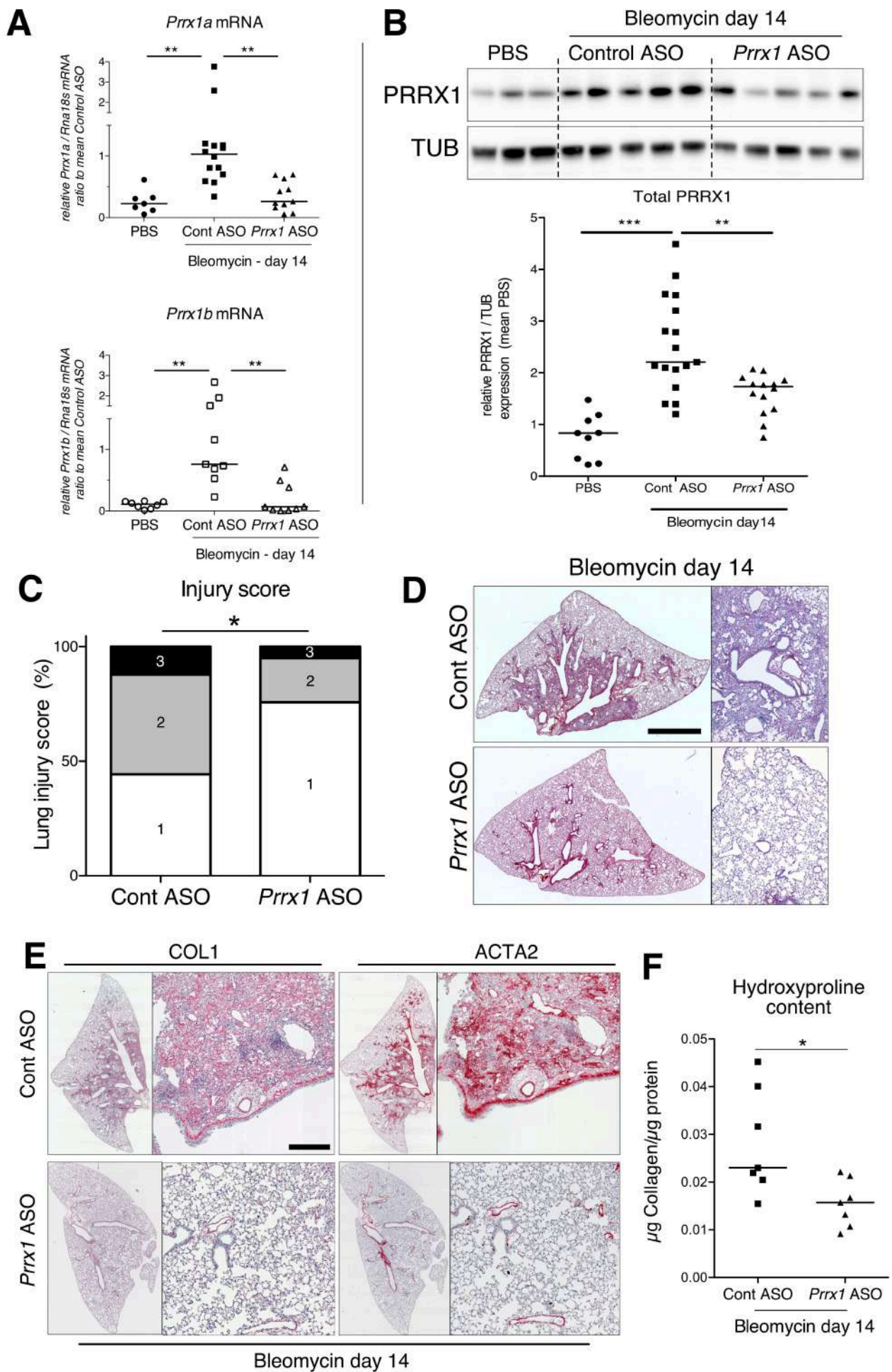


Figure 7

Figure 7: PRRX1 inhibition attenuates lung fibrosis in bleomycin murine model.

(A) Dot plots with median showing the mRNA expression of *Prrx1a* (black) and *Prrx1b* (white) isoforms at day 14 (n=8) in PBS (circle) mice and bleomycin mice treated with control ASO (square, n=14) or *PRRX1* ASO (triangle, n=11). (B) Immunoblot showing PRRX1 expression at day 14 in PBS mice and bleomycin mice treated with Control ASO or *Prrx1* ASO. TUB was used as loading control. The quantification of PRRX1 expression relative to TUB at day 14 in PBS mice (circle, n=9) and bleomycin mice treated with Control ASO (square, n=16) or *Prrx1* ASO (triangle, n=14) is displayed as dot plot with median on the lower panel. (C) Injury score at day 14 of bleomycin mice treated with *Prrx1* ASO or Control ASO. (D) Representative immunohistochemistry images (n=7 per group) showing picrosirius staining (red) at day 14 in bleomycin mice treated with Control ASO or *Prrx1* ASO. (E) Representative immunohistochemistry images (n=7 per group) showing COL1 (left panel) and ACTA2 (right panel) staining (red) at day 14 in bleomycin mice treated with Control ASO or *Prrx1* ASO. Nuclei were counterstained with hematoxylin. (F) Dot plot with median showing the relative Collagen content as measured by hydroxyproline at day 14 in bleomycin mice treated with control ASO (square, n=7) or *PRRX1* ASO (triangle, n=7). (Scale bar: 80µm in low magnification images and 40µm in high magnification ones); (Abbreviations: Control (Cont), Antisense oligonucleotide (ASO)). Kruskal-Wallis test with Dunns post-test (A and B), Fisher's exact test (C) and Mann Whitney U test (F); *p≤0.05, **p≤0.01, ***p≤0.001

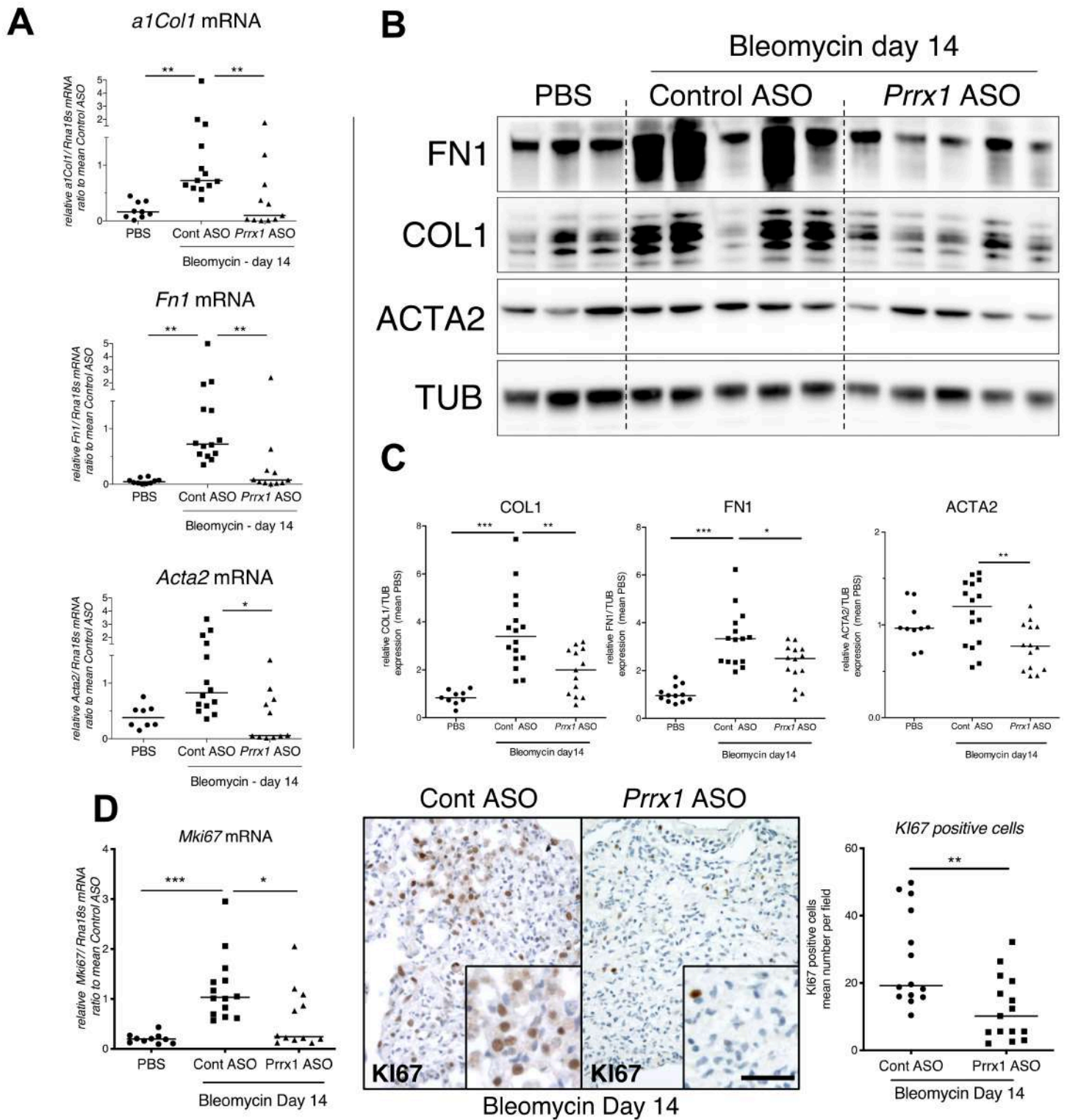


Figure 8

Figure 8: PRRX1 inhibition decreases fibrosis markers in bleomycin mice.

(A) Dot plots with median showing the mRNA expression of *Col1a1*, *Fn1* and *Acta2* at day 14 in PBS mice (circle, n=9) and bleomycin mice treated with Control ASO (square, n=14) or *Prrx1* ASO (triangle, n=11). (B) Immunoblot showing FN1, COL1 and ACTA2 expression at day 14 in PBS mice and bleomycin mice treated with Control ASO or *Prrx1* ASO. TUB was used as loading control. (C) Quantification of FN1, COL1 and ACTA2 relative expression to TUB at day 14 in PBS mice (n=9) and bleomycin mice treated with Control ASO (n=16) or *Prrx1* ASO (n=13) (D) Left panel: dot plots with median showing *Mki67* mRNA expression of at day 14 in PBS mice (circle, n=10) and bleomycin mice treated with Control ASO (square, n=14) or *Prrx1* ASO (triangle, n=14). Middle panel: representative immunohistochemistry pictures (n= 14 per group) showing Ki67 staining (brown) in bleomycin treated with Control ASO (left) or *Prrx1* ASO (right) mice at day 14. The quantification of the number of Ki67 positive cells per high magnification field is shown on the right as dot plots with median. (Scale bar: 40µm in low magnification images and 20µm in high magnification ones). Abbreviations: Control (Cont), Antisense oligonucleotide (ASO)). Kruskal-Wallis test with Dunns post-test (A, C, D) and Mann Whitney U test (D); *p≤0.05, **p≤0.01, ***p≤0.001

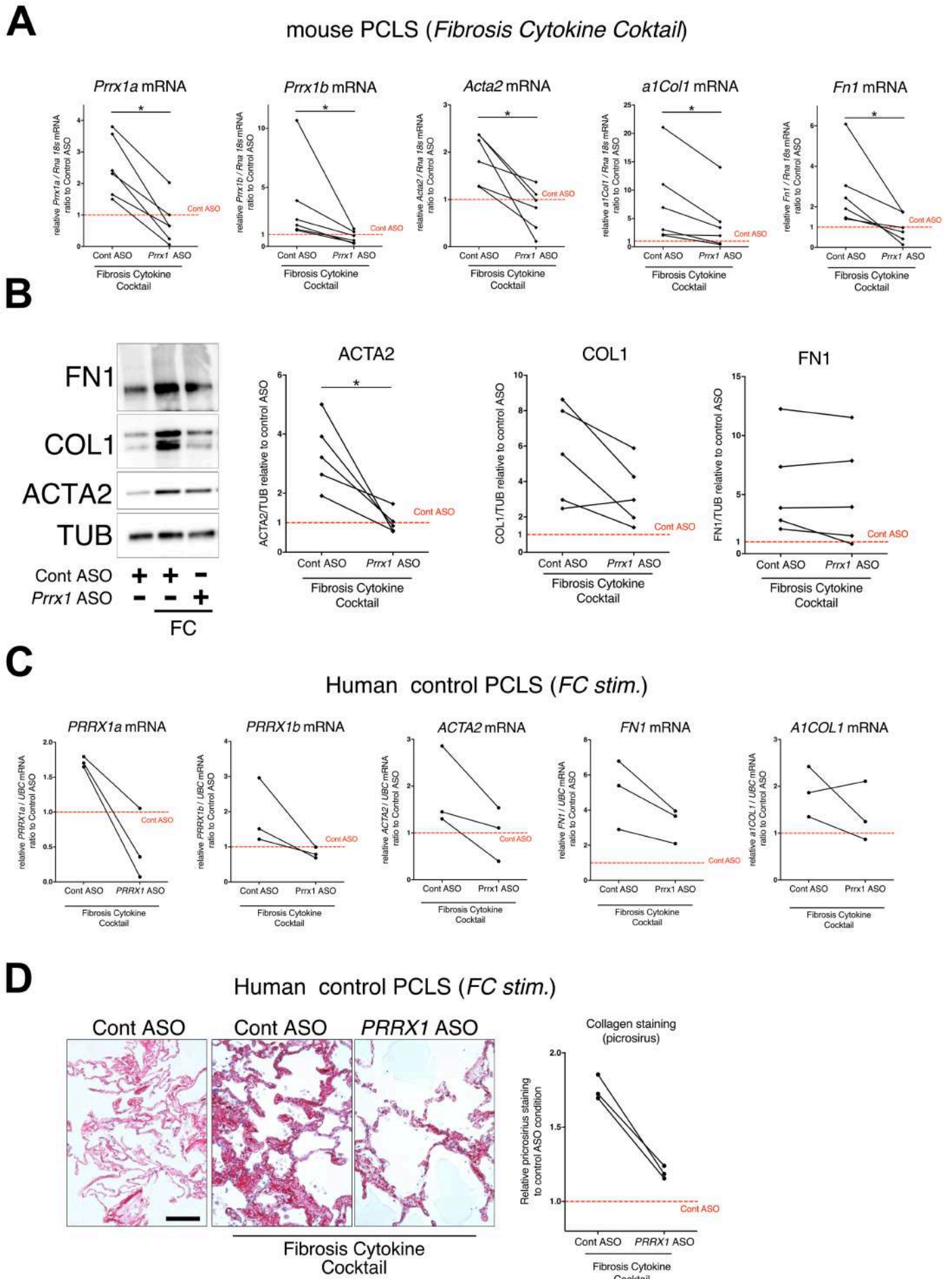


Figure 9

Figure 9: *PRRX1* ASO attenuates lung fibrosis in mouse and Human Precision-cut Lung slices (PCLS)

(A) Before-after plots showing the mRNA expression of *Prrx1a*, *Prrx1b*, *Acta2*, *a1Col1* and *Fn1* (n=6) relative Control ASO alone condition (red dashed line) in mouse PCLS stimulated with fibrosis cytokine cocktail (FC) and then treated either with control ASO or *PRRX1* ASO. (B) Representative immunoblot showing FN1, COL1 and ACTA2 expression relative to control ASO alone condition (red dashed line) in mouse PCLS stimulated with FC and then treated either with control or *Prrx1* ASO. The corresponding quantifications of ACTA2, COL1 and FN1 expression ratio to Tubulin are displayed as before-after plots on the right. Note that COL1 expression was decreased in 4 out 5 experiments. (C) Before-after plots showing the mRNA expression of *PRRX1a*, *PRRX1b*, *ACTA2*, *A1COL1* and *FN1* (n=3) relative Control ASO condition (red dashed line) in Human PCLS treated either with control ASO or *PRRX1* ASO in presence or absence of FC. *A1COL1* upregulation was lessened in 2 out 3 experiments while *ACTA2* and *FN1* levels were decreased in 3 out of 3 experiments. (D) Representative picrosirius staining (n=3) in Human PCLS treated with control ASO alone (left panel, basal condition) or after stimulation with Fibrosis Cytokine cocktail and treated with either control (middle panel) or *PRRX1* (right panel) ASO. Nuclei were counterstained with hematoxylin. The quantification of picrosirius staining relative to control ASO alone (red dashed line) is showed on the right (Before-after plot). (Scale bar: 50µm) Abbreviations: Precision-Cut Lung Slices (PCLS), Fibrosis Cytokine Cocktail (FC), Control (Cont), Antisense oligonucleotide (ASO), Stimulation (stim.). Wilcoxon test *p≤0.05.

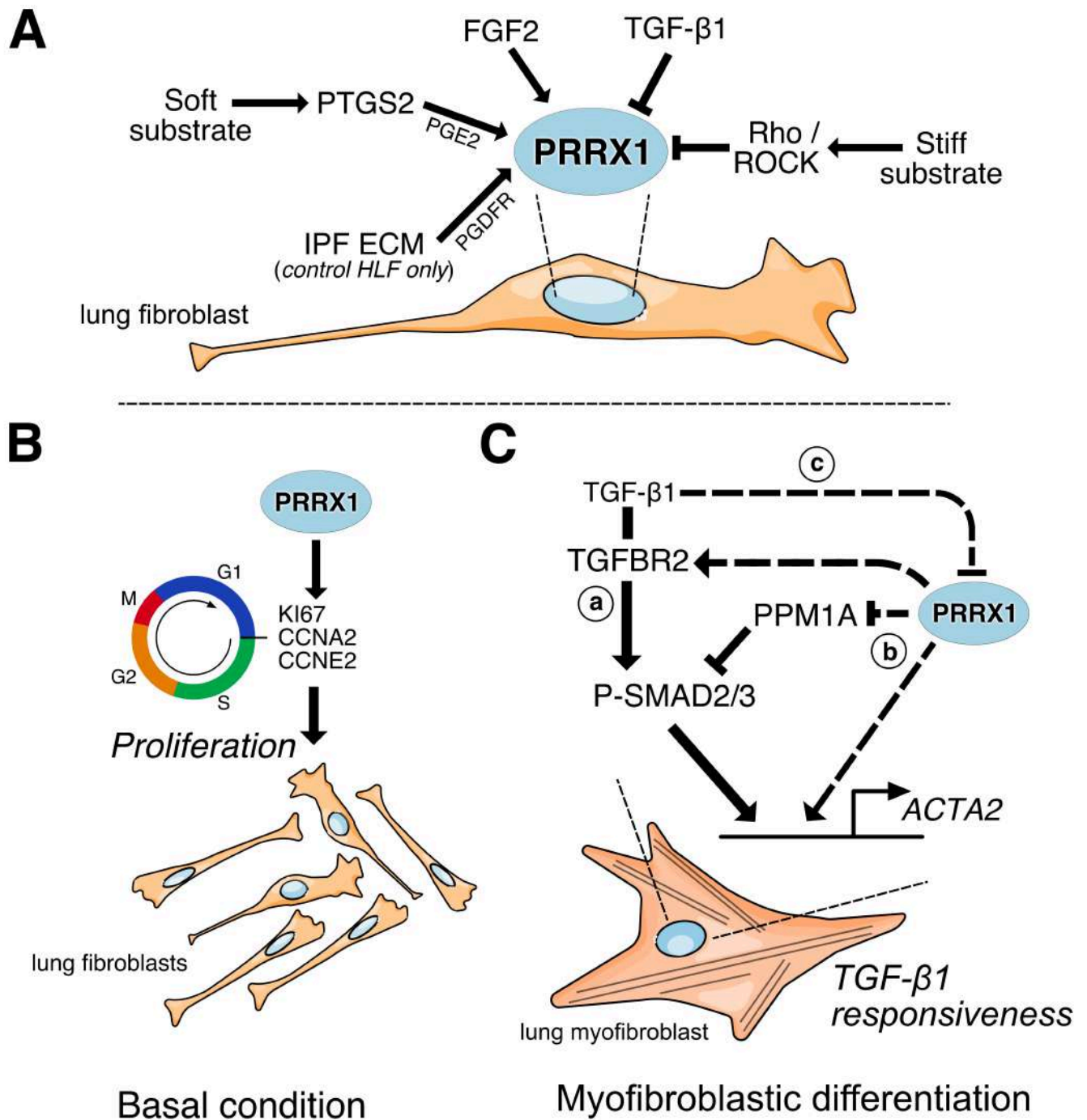


Figure 10

Figure 10: summary sketch of PRRX1 regulation and functions in lung fibroblasts.

(A) Regulation of *PRRX1* TF expression in lung fibroblasts. On one hand, *PRRX1* expression was up-regulated by proliferative and anti-fibrotic pathways and signals: FGF2, PGE2 and soft culture substrate (in a *PTGS2* dependent-manner). IPF fibroblast-derived matrix also increased *PRRX1* TFs expression in a *PDGFR* dependent manner in control primary lung fibroblasts only. On the other hand, stiff culture substrate (in a Rho/ROCK dependent manner) and TGF- β 1 stimulation, which both promote myofibroblastic differentiation, decreased *PRRX1* TF expression levels in both control and IPF fibroblasts seeded on plastic. **(B)** Model of *PRRX1* function in lung fibroblasts at steady state. In complete growth medium, *PRRX1* TFs influence cell cycle progression by regulating key factors associated with cycle progression during the G1 and S phases (KI67, Cyclin A2 and E2). *PRRX1* was detected in the promoter regions of those genes by chromatin immunoprecipitation (ChIP). **(C)** Model of *PRRX1* function in lung fibroblasts during myofibroblastic differentiation. (a) TGF- β 1 stimulation of lung fibroblasts will trigger their differentiation into myofibroblasts by promoting the phosphorylation of SMAD2 and SMAD3. P-SMAD2/3 will then induce the upregulation of *ACTA2* expression. (b) In presence of *PRRX1*, the expression of the serine / threonine phosphatase PPM1A is downregulating (*PRRX1* TFs binding to PPM1A promoter region was demonstrated by ChIP) and *TGFBR2* expression is also maintained. Thus, the phosphorylation of SMAD2 and SMAD3 is therefore not impacted. The effect of *PRRX1* TFs upon *ACTA2* loci could be also direct since *PRRX1* binding to *ACTA2* regulatory sequences was demonstrated by ChIP and has been previously reported in other mesenchymal cells ²⁹. (c) During myofibroblastic differentiation, the expression of *PRRX1* TFs was then decreased after TGF- β 1 treatment for 48h (not at 24h) on plastic. This negative feedback loop could limit cell-responsiveness to long exposure of TGF- β 1 by upregulating the expression of PPM1A and downregulating *TGFBR2* levels. *Abbreviations: IPF (Idiopathic Pulmonary Fibrosis), HLF (Human Lung Fibroblasts), ECM (Extracellular matrix), G1 (Gap 1 phase 1), S (Synthesis / Replicative phase), G2 (Gap phase 2), M (Mitosis), CCNA2 (Cyclin A2), CCNE2 (Cyclin E2).*